THE JOURNAL OF BIOLOGICAL CHEMISTRY VOL. 289, NO. 51, pp. 35042–35060, December 19, 2014
Published in the U.S.A.

The *Drosophila* Tis11 Protein and Its Effects on mRNA Expression in Flies*

Received for publication, July 1, 2014, and in revised form, October 21, 2014 Published, JBC Papers in Press, October 23, 2014, DOI 10.1074/jbc.M114.593491

Youn-Jeong Choi[‡1], Wi S. Lai[‡1], Robert Fedic[§2], Deborah J. Stumpo[‡], Weichun Huang[¶], Leping Li[¶], Lalith Perera[‖], Brandy Y. Brewer[**], Gerald M. Wilson[**], James M. Mason[§], and Perry J. Blackshear[‡ ‡‡3]

From the Laboratories of [‡]Signal Transduction, [§]Molecular Genetics, [¶]Biostatistics, and [‖]Structural Biology, NIEHS, National Institutes of Health, Research Triangle Park, North Carolina 27709, the [**]Department of Biochemistry and Molecular Biology, University of Maryland, Baltimore, Maryland 21201, and the [‡‡]Departments of Medicine and Biochemistry, Duke University Medical Center, Durham, North Carolina 27710

Background: Insects generally express a single tristetraprolin family member, zinc finger proteins that promote mRNA decay.
Results: The *Drosophila* protein, Tis11, can promote mRNA decay in cells, and its deficiency in flies results in accumulation of certain mRNAs.
Conclusion: Tis11 deficiency in *Drosophila* results in increases of potential target transcripts.
Significance: Tis11 can affect post-transcriptional gene expression in adult flies by regulating mRNA decay.

Members of the mammalian tristetraprolin family of CCCH tandem zinc finger proteins can bind to certain AU-rich elements (AREs) in mRNAs, leading to their deadenylation and destabilization. Mammals express three or four members of this family, but *Drosophila melanogaster* and other insects appear to contain a single gene, *Tis11*. We found that recombinant *Drosophila* Tis11 protein could bind to ARE-containing RNA oligonucleotides with low nanomolar affinity. Remarkably, co-expression in mammalian cells with "target" RNAs demonstrated that Tis11 could promote destabilization of ARE-containing mRNAs and that this was partially dependent on a conserved C-terminal sequence resembling the mammalian NOT1 binding domain. *Drosophila* Tis11 promoted both deadenylation and decay of a target transcript in this heterologous cell system. We used chromosome deletion/duplication and *P* element insertion to produce two types of Tis11 deficiency in adult flies, both of which were viable and fertile. To address the hypothesis that Tis11 deficiency would lead to the abnormal accumulation of potential target transcripts, we analyzed gene expression in adult flies by deep mRNA sequencing. We identified 69 transcripts from 56 genes that were significantly up-regulated more than 1.5-fold in both types of Tis11-deficient flies. Ten of the up-regulated transcripts encoded probable proteases, but many other functional classes of proteins were represented. Many of the up-regulated transcripts contained potential binding sites for tristetraprolin family member proteins that were conserved in other *Drosophila* species. Tis11 is thus an ARE-binding, mRNA-destabilizing protein that may play a role in post-transcriptional gene expression in *Drosophila* and other insects.

The control of mRNA turnover rates is critical for the physiological regulation of gene expression. The rates of turnover of an individual mRNA can vary greatly under different physiological conditions and in response to a variety of stimuli. Factors contributing to mRNA lability include *cis*-acting sequences within mRNA, often in the 3′-untranslated regions (UTRs). One such category of instability-promoting sequences is the AU-rich element (ARE),[4] first described (1) as a sequence within the 3′-UTR of the mammalian granulocyte-macrophage colony-stimulating factor (GM-CSF) mRNA. Numerous proteins that can bind to these elements have been identified as potential mRNA-stabilizing or -destabilizing factors (2, 3). One of the best characterized is tristetraprolin (TTP), an ARE-binding protein that can promote the instability of mRNAs, such as those encoding tumor necrosis factor (TNF) and GM-CSF itself as well as an increasing list of other binding targets whose identities have been established in part by studying the responses of transcripts in cells derived from TTP knock-out mice (4–6).

TTP belongs to a small family of four related proteins in rodents, all of which have as their characteristic mRNA binding element a tandem zinc finger (TZF) domain, with identical interfinger spacing of two $CX_8CX_5CX_3H$ zinc fingers (7). The 74-amino acid TZF domain of the proteins binds to characteristic ARE sequences with low nanomolar affinity, with the preferred binding site being UUAUUUAUU (8, 9); each finger binds to a UUAU half-site with virtually superimposable structures (10). In mice, disruption of the gene encoding TTP, *Zfp36*, demonstrated that TTP is an anti-inflammatory protein, whose absence leads to a severe, systemic inflammatory syndrome with erosive arthritis (11). Disruption of the gene encoding the second family member, *Zfp36-like 1* (*Zfp36l1*), showed that this gene is necessary for normal allantoic fusion with the chorion and establishment of the normal feto-placental circulation (12). The third mouse family member, *Zfp36l2*, is important for the

* This work was supported, in whole or in part, by the National Institutes of Health (NIH), NIEHS, Intramural Research Program and by NIH Grant R01 CA102428 (to G. M. W.). This work was also supported by an Oliver Smithies Visiting Professorship at Balliol College, Oxford (to P. J. B.).
[1] Both authors contributed equally to this work.
[2] Present address: GeneTiCA s.r.o., Prague 108 00, Czech Republic.
[3] To whom correspondence should be addressed: NIEHS, National Institutes of Health, 111 Alexander Dr., F1-13, Research Triangle Park, NC 27709. Tel.: 919-541-4926; Fax: 919-541-4571; E-mail: black009@niehs.nih.gov.

[4] The abbreviations used are: ARE, AU-rich element; TTP, tristetraprolin; TZF, tandem zinc finger; EGFP, enhanced green fluorescent protein; 293 cells, human embryonic kidney 293 cells; MLP, MARCKS-like protein; mRNASeq, deep sequencing of mRNA.

proliferation of early embryos past the two-cell stage (13) and is essential for hematopoiesis (14). Finally, in rodents, *Zfp36l3* encodes a cytosolic, placenta-specific protein (7, 15). Each protein behaves like TTP in co-transfection assays of TTP-induced mRNA instability and cell-free assays of mRNA decay (16); however, the presumed physiological targets for the other family members are largely unknown. Most vertebrates, including mammals, amphibians, and reptiles, express orthologues of the first three family members (TTP or ZFP36, ZFP36L1, and ZFP36L2). Birds appear to lack TTP (17), and amphibians and fish express one additional protein that does not have a direct mammalian orthologue (*Xenopus* C3H-4 (18)). We anticipate that various species will use proteins of this type in complex ways to regulate mRNA stability. However, it is impossible to predict which, if any, of the four or more physiological systems primarily regulated by the mammalian proteins will translate into non-vertebrate organisms with fewer family members.

Proteins with similar TZF domains have been identified in other eukaryotes, including plants, protists, nematodes, yeasts, and insects (19). At least one of the two such proteins expressed in *Saccharomyces cerevisiae* affects the stability of a collection of transcripts involved in regulating iron metabolism, apparently also by binding to ARE elements that are similar to their mammalian counterparts (20, 21). In *Schizosaccharomyces pombe*, the single family member, Zfs1p, also binds to and promotes the decay of ARE-containing mRNAs (22, 23), but in this case, the major phenotypic effect of the protein is to prevent abnormal cell-cell interactions, and iron metabolism appears to be unaffected. This evidence strongly suggests that at least some of the functions of proteins from this family have been conserved in eukaryotes, such as the ability to bind to and destabilize ARE-containing mRNAs, but that these proteins can be used for different physiological purposes in different species.

Most insect genomes appear to contain only a single gene expressing proteins of this type. In *Drosophila melanogaster*, for example, the protein product of the *Tis11* locus contains a TZF domain with identical critical residues and spacing to the mammalian members of the TTP family (24). The effects of the encoded protein, Tis11, have been studied recently in *Drosophila* S2 cells, with an emphasis on the possible relevance to *Drosophila* innate immunity, based on the analogy with TTP itself (25–30). However, very little is known about the physiological role of *Tis11* in intact flies. Because of the apparent expression of only a single such gene in most if not all insect species, the genetic tractability of *Drosophila*, and the economic and medical importance of many other insects, we have begun to explore the physiological role of the Tis11 protein in flies. We show here that Tis11 resembles the mammalian proteins in many respects, in that it exhibits high affinity ARE-binding through its TZF domain and has mRNA-deadenylating and -destabilizing properties that are in part due to the presence of a C-terminal potential Not1 binding domain. Two different genetic models of loss of function in adult flies suggest that, as expected, it can regulate post-transcriptional gene expression in *Drosophila*. Strikingly, the transcripts identified in adult flies as potential Tis11 targets were almost entirely different from those identified as targets in S2 cells, suggesting that both approaches may be complementary in elucidating the physiological role of this protein in insects.

MATERIALS AND METHODS

Expression Plasmids

CMV.dTis11—The template used to amplify the Tis11 protein coding fragment was an expressed sequence tag clone purchased from the IMAGE consortium (GenBank™ accession number AI512677). This clone contained the entire predicted *D. melanogaster* Tis11 variant A protein coding sequence (GenBank™ accession number NP_511141.2). The PCR primers used were 5′-ggtaccACAAAATGTCTGCTGATATTCTG-3′ (5′) and 5′-ctcgagTTAGAGTCCCAAATTGGACTGCTGC-3′ (3′), where the capital letters correspond to the *Tis11* sequences and the lowercase letters correspond to the recognition sites for Asp718 (the 5′ primer) and XhoI (the 3′ primer). The PCR product was digested with Asp718 and XhoI and ligated into the vector CMV.BGH3′/pBS+ (31).

CMV.dTis11.HA/His—In this construct, the hemaglutinin-His_6 (HA/His_6) epitope tags were linked to the last amino acid of the Tis11 protein by the polymerase chain reaction primer-overlapping mutagenesis technique (32), and a BamHI site was created between the Tis11 C terminus and the epitope tag. The fusion cDNA was then ligated into the Asp718 and XhoI sites of the vector CMV.BGH3′/pBS+. Key cysteine and histidine residues in the Tis11 TZF domain were mutated to other amino acids to create potential non-RNA-binding mutants, using the PCR primer-overlapping mutagenesis technique. The primer representing the upper strand sequence used in the mutation of cysteine 150 to a serine (C150S) was 5′-GCCGGAGAA<u>TCC</u>AAGTACGGCG-3′, in which the bases encoding serine are underlined. To mutate histidine 198 to a glutamine (H198Q), the primer representing the upper strand sequence was 5′-CACTTTGTT<u>CAG</u>AATGCGGAC-3′, with the underlined bases encoding glutamine.

CMV.dTis11.GFP—An Asp718-BamHI fragment from the construct CMV.dTis.HA/His, which contained the entire protein coding region except the stop codon (with or without the mutated key cysteine and histidine residues), was ligated into the vector CMV.EGFP.BGH3′/BS+ for the expression of the Tis11.GFP fusion protein. The vector CMV.EGFP.BGH3′/BS+ was made by ligating a BamHI-NotI fragment from pEGFP-N1 (Clontech), containing the protein coding region for EGFP, into the BamHI and NotI sites of CMV.BGH3′/pBS+.

CMV.HA.dTis11 and Its C-terminal Truncation Mutants—These constructs were used to study the involvement of the conserved C-terminal domain in the ability of Tis11 to destabilize ARE-containing mRNAs. The conserved C-terminal motif of nine amino acids, RLP(I/V)FNR(I/L)S, recently implicated in the binding of human TTP to NOT1 (33), is located at 414–422 of the Tis11 isoform A (GenBank™ accession number NP_511141.2). A 5′ primer containing the Asp718 restriction enzyme site and encoding the Tis11 isoform A residues 1–7, 5′-ggtaccATGTCTGCTGATATTCTGCAG-3′, was used to create the following expression constructs. For full-length CMV.HA.Tis11, the 3′ primer used for plasmid CMV.dTis11 was used. For the truncation plasmid CMV.HA.Tis11Δ414–422,

a pair of complementary primers were used that encoded the sequences for Tis11 residues, ^{408}QQEDTP-deletion-SGVEAY^{428}, in combination with the 5′ and 3′ primers described for the CMV.HA.dTis11 plasmid, using the PCR primer-overlapping technique (32). The upper strand sequence was 5′-CAGCAGGAGGATACGCCC,TCCGGTGTGGAGGCCTAC-3′, with the comma denoting the site of the deletion.

For the truncation plasmid CMV.HA.Tis11Δ414–436, a 3′ PCR primer containing the sequences for residues 406–413, the stop codon, and the XhoI restriction enzyme was used. The PCR products were digested with Asp718 and XhoI and ligated into the vector CMV.HA.BGH3′/pBS+,[5] in frame with the HA tag at the Tis11 N terminus. The RNA-degrading activities of Tis11 expressed from these constructs were assessed by co-transfecting them with the Mlp-TNF3′ target plasmid, in which a portion of the mouse *Mlp* promoter and the protein coding region of the mouse Mlp mRNA is followed by a 3′-UTR consisting of a portion of the mouse Tnf mRNA 3′-UTR, as described in detail previously (15). The mouse *Mlp* promoter is very sensitive to actinomycin D, in contrast to the CMV promoters used for the other expression plasmids used in this study.

For bacterial expression, the cDNA clone CMV.dTis11 was used as a template for PCR; the amplified fragment containing the entire open reading frame was cloned into the expression vector pET21a in frame with a His_6 tag on the 3′-end by standard procedures (Abgent, San Diego, CA). The resulting expression plasmid was used for the expression in and purification of the Tis11-His_6 fusion protein from *E. coli* using nickel affinity columns (Abgent). This purified protein was used either in gel shift RNA binding studies, using a mouse Tnf mRNA-based cDNA probe as described (31), or in quantitative fluorescence anisotropy binding studies as described below. In addition, a total of 825 μg of purified protein per rabbit was used to produce polyclonal antisera according to standard procedures (Covance, Princeton, NJ).

RNA-Protein Binding Affinity

Quantitative measurements of RNA-protein binding affinity were performed using a fluorescence anisotropy-based assay essentially as described (34). Briefly, a fluorescein-tagged RNA substrate (Fl-ARE, with sequence Fl-AUUUAUUUAUUUA; 0.2 nM) containing a single high affinity binding site for the human TTP TZF domain (35) was incubated at 25 °C with varying concentrations of recombinant Tis11 in a final volume of 100 μl containing 10 mM Tris·HCl (pH 8.0), 100 mM KCl, 2 mM dithiothreitol, 0.1 μg/μl bovine serum albumin, 5 μM $ZnCl_2$, and 0.2 μg/μl heparin. Fluorescence anisotropy was measured with a Beacon 2000 fluorescence polarization system (Panvera, Madison, WI) using fluorescein excitation (λ_{ex} = 490 nm) and emission (λ_{em} = 535 nm) filters. Protein binding increases the measured anisotropy of the fluorescein-conjugated RNA, based on restriction of segmental motion and rotational correlation time (36). Tis11 binding did not influence the fluorescence quantum yield of the Fl-ARE substrate (data not shown), permitting the bimolecular association constant (K_a) to be resolved from binding reactions across a titration of protein ([Tis11]) using Equation 1 (34),

$$A_t = \frac{A_R + A_{PR}K_a[\text{Tis11}]}{1 + K_a[\text{Tis11}]} \quad \text{(Eq. 1)}$$

where A_t represents the total measured anisotropy, and A_R and A_{PR} represent the intrinsic anisotropy values of the free and protein-associated Fl-ARE substrates, respectively. A_R was measured as the anisotropy of the Fl-ARE substrate in the absence of protein ($n \geq 3$), whereas all other constants were solved by non-linear least squares regression of A_t *versus* [Tis11] using PRISM version 3.0 (GraphPad, San Diego, CA). Complex dissociation constants (K_d) were resolved using $K_d = 1/K_a$.

Structural Modeling Studies

Tis11-RNA Complex—An initial model of the TZF domain of *D. melanogaster* Tis11 (amino acids 133–202 from GenBank™ accession number AAF48194.2) was created using the RNA-bound structure of the TZF domain of ZFP36L2 (TIS11d) (Protein Data Bank entry 1RGO (10)). Necessary mutations were introduced into the sequence of human ZFP36L2 using Coot (37) to generate a model of the Tis11 TZF domain in its RNA-bound form (with two CCCH coordinated zinc ions) and energy-minimized using the program Amber.12. The RNA-bound Tis11 TZF complex was solvated in a box of water (about 9500 water molecules). Prior to equilibration, the solvated system was subjected to 1) 100-ps belly dynamics runs with fixed peptide, 2) minimization, 3) low temperature constant pressure dynamics at fixed protein to assure a reasonable starting density, 4) minimization, 5) stepwise heating molecular dynamics at constant volume, and 6) constant volume molecular dynamics for 1 ns. A final unconstrained molecular dynamics trajectory was calculated at 300 K under constant volume (15 ns, time step 1 fs) using PMEMD (Amber.12) to accommodate long range interactions. The force field parameters were taken from the FF03 force field (38) for the protein and the PARMBSC0 force field (39) for the RNA. The charge on zinc ions was +2, whereas cysteine coordinated with zinc carried a −1 charge. His coordinated to zinc remained neutral. The van der Waals parameters of zinc were adjusted to yield Zn–S and Zn–N distances between 2.25 and 2.50 Å during the simulations. No specific constraints were applied to maintain the zinc coordination. Images of molecular models were created using VMD.1.9.1 (40).

Human TTP (or Tis11) Bound to Human NOT1 or Drosophila Not1—Using the x-ray crystal structure (Protein Data Bank entry 4J8S) of human TTP bound to human NOT1 (residues 820–999) (33), an initial model for the conserved Tis11 C-terminal domain bound to the TTP binding domain of human NOT1 was created. Necessary mutations were carried out using the program Coot (37). Using the coordinates of human TTP bound to human NOT1 as a template, Coot was employed to construct an initial model of Tis11 bound to *Drosophila* Not1. The new models of Tis11 bound to human NOT1, Tis11 bound to *Drosophila* Not1, and the original model of human TTP bound to human NOT1 (33) were then solvated separately in a

[5] W. S. Lai and P. J. Blackshear, unpublished data.

box of water, and the solvated systems were subjected to the protocol described above, followed by a long molecular dynamics simulation at $T = 300$ K using the "PMEMD" module of the program Amber.12. The final snapshots of the bound solution structure (after 25 ns) were selected for comparison.

Cell Transfections

For mammalian cell transfection experiments, human embryonic kidney 293 cells (referred to as 293 cells) were transfected with the plasmids described above that expressed either the epitope-tagged normal Tis11 protein, its mutant derivatives, or the untagged protein and its C-terminal truncations, driven by the CMV promoter. In one case, 293 cells were co-transfected with the plasmids expressing the Tis11 fusion proteins along with a somewhat shortened version of the mouse Tnf mRNA, which contains several potential TTP binding sites but excludes other AU-rich sequences, as described in detail previously (31). This represents one assay for the mRNA-destabilizing activities of TTP family member proteins. A plasmid encoding human TTP was transfected in parallel experiments as a positive control. In this case, the assay readout consisted of Northern blots probed with radiolabeled probes for TNF, as described (31); in addition, expression levels of TTP and Tis11 mRNA were determined by Northern blotting, using total cellular RNA isolated from the transfected cells as described (31).

In another series of transfection experiments, CMV-driven Tis11 and its C-terminal truncations were co-transfected with constructs in which an Mlp-Tnf 3′-UTR fusion transcript was driven by the mouse *Mlp* promoter, as described (15). The ability of Tis11 constructs to promote decay of the Mlp-Tnf3′ fusion mRNA was assessed by Northern blotting with an Mlp cDNA probe, as described (15).

In other transfection experiments, plasmids encoding either epitope-tagged human TTP or Tis11 were transfected into 293 cells, and the soluble cellular supernatants were used in RNA gel shift assays as described (31). This assay used a radiolabeled probe based on the core ARE sequence of the mouse Tnf 3′-UTR (31).

Cell-free Deadenylation Assays

In these assays, performed essentially as described (41), the RNA (8 μg/tube) was incubated in 10 μl of 50 mM KCl without (−) or with (+) 0.6 μg of dT_{12-18} at 95 °C for 5 min, followed by another 30 min at 25 °C. A 15-μl aliquot of buffer was then added to each tube, without (−) or with (+) 1 unit of RNase H (New England Biolabs) and incubated for 45 min at 37 °C. The final incubation buffer contained 30 mM Tris-HCl (pH 8.3), 65 mM KCl, 4.8 mM $MgCl_2$, 6 mM DTT, and bovine serum albumin (0.5 μg/μl).

RNA Decay Assays

Each plate of 293 cells was co-transfected with 3 μg of the Mlp-Tnf3′ plasmid and 2 μg of vector (BS+) DNA. In addition, 5 ng of an EGFP construct was added along with 5 ng of CMV/BS+ vector DNA (control group), 10 ng of CMV.DTis11.HA/His_6 (WT Tis11 group), or a construct encoding the Tis11 mutant H198Q (mutant group). Twenty-four h after removing the transfection mixture, RNA was isolated from three plates of cells from each group, and actinomycin D (5 μg/ml) was added to the rest of the plates. At each indicated incubation period, three plates of cells from each group were used for RNA isolation, and this was used for Northern blotting with a mouse Mlp cDNA probe. These were quantitated using a PhosphorImager and ImageQuant software (GE Healthcare). The PhosphorImager volume of the transfected-expressed Mlp-Tnf3′ mRNA at each gel lane was normalized with the volume of the endogenous MLP mRNA in the same lane. Similar transfection experiments were performed five times.

Drosophila Stocks

The *P* element insertion stock *w* P*[*EP*]*Tis11*^{G147} (referred to below as *G147*) was purchased from GenExel (Daejeon, South Korea); this *P* element was described by GenExel as within the first exon of *Tis11*. *Df(1)Tis11-IE35* (hereafter known as *IE35*) was identified in an imprecise excision screen performed by mobilizing the *P* element in *G147* with the Δ2-3 transposase, followed by screening for lethals over *Df(1)N105*, obtained from the Bloomington Drosophila Stock Center. In this screening, with the help of a *mus309* allele mutation, large deletions were created. *Dp(1;Y)BSC5* (hereafter known as *BSC5*) is a Y chromosome bearing an X chromosome duplication from 11B9 to 11D5 and a second duplication bearing y^+ and was obtained from the Bloomington Drosophila Stock Center.

We also obtained the *P* element insertion stock *w* P*[*EP*]-*Tis11*^{G1183}/*FM7c* (referred to below as *G1183*) from GenExel. This *P* element was also described as within the first exon of the *Tis11* gene. *G1183* was reported by GenExel to be homozygous lethal, and the orientation of the UAS sequence within the *EP* element (42) should drive transcription in the opposite direction relative to the Tis11 transcript when exposed to *Gal4* drivers. *G147* was described as viable and is expected to drive transcription in the 5′-3′ direction relative to *Tis11*. The *P* element insertion sites and orientation were confirmed by direct sequencing from both directions and are as follows. For *G147*, the insertion site is between bp 12553436 and 12553437 of the X chromosome sequence NC_004354.3 or between bases 42 and 43 of the Tis11 mRNA sequence NM_078586.3. For *G1183*, the *P* insertion site was between bp 12553497 and 12553498 of the X chromosome sequence NC_004354.3 or between bases 103 and 104 of the Tis11 mRNA sequence NM_078586.3.

The original lethal *G1183* chromosome became viable during maintenance in our facility and was termed *G1183v*. We therefore tried to eliminate possible mutation(s) other than the *P* element in the original chromosome by allowing meiotic recombination with a chromosome marked with w^{1118}. The resulting viable recombinant chromosome was termed "*G1183rec*." This chromosome still contained the w^+ *P* element but was viable, suggesting that the lethality of the original *G1183* chromosome resulted from one or more additional mutations outside the *Tis11* locus. These flies were then backcrossed to *y* w^{67c23} flies for 10 generations to form the *G1183* and control flies used for mRNASeq in this paper.

Genomic and Real-time PCR

To determine the location and extent of the deletion in the *IE35* allele, *IE35* homozygous early larvae (GFP−) were collected, along with GFP+ larvae containing the *FM7* balancer. Genomic DNAs were purified using DNAzol reagent (Invitrogen) according to the manufacturer's instructions. Primers used for PCR were as follows: Smr, 5′-AACTGGTCCACCACGCTCAA-3′ (forward) and 5′-GGCAACGGAGCATGAACGAA-3′ (reverse); ade5, 5′-TCGTTTGTGAACTCAAAGCCCACG-3′ (forward) and 5′-TAGCTCGAACTTGGCGGAGACAAT-3′ (reverse); CG3812 5′- CTGCATCATTGTGGCCAATCACCA-3′ (forward) and 5′-GCTTCTTGATGCGCCGGTTAACAT-3′ (reverse); CG32647, 5′-ACTGCAACTGCGTATCAACAACGC-3′ (forward) and 5′-AGGCAGGCTGACATTGTTATGGGA-3′ (reverse); Pde9, 5′-GACAAGTGGCGCAAATGGTCAAGT-3′ (forward) and 5′-TGGAAATGGCGAATGCATAGCTGC-3′ (reverse); CG4661, 5′-ATTCCACCTCCTACAGCTGCCTTT-3′ (forward) and 5′-TCCTGGCGTCTCATTATTTGGGCA-3′ (reverse); CG32650, 5′-TCTCTGCATACTCCAAGCGAGACT-3′ (forward) and 5′-GCCTTGCGAGAACTGCAATGGAAT-3′ (reverse).

For determination of the *BSC5* duplication endpoints, genomic DNAs were purified from *IE35/BSC5* and control w^{1118}*/BSC5* male flies. Sequences 3′ of the *Tis11* coding sequences were selected for amplification using PCR. Primers used for PCR were 5′-CGAATGTCGATCTTTGTATGCGTCGG-3′ (forward) and 5′-CTCTTTCACCGGCCGTTTGTTTGT-3′ (reverse).

Real-time RT-PCR

For adult flies, total cellular RNA was isolated from 0–1-day-old *G1183v* and *G1183rec* males and 1–5-day-old *IE35/BSC5* males previously frozen at −80 °C, using the Illustra RNAspin kit (GE Healthcare) according to the manufacturer's instructions. Total RNA was reverse transcribed into first-strand cDNA using the ABI/Prism High Capacity cDNA Archive Kit (Applied Biosystems, Foster City, CA). Each SYBR Green reaction contained 2 μl of cDNA, 5 μl of Power SYBR Green PCR Master Mix (Applied Biosystems), 0.4 μl each of 10 μM forward and reverse primers, and 2.2 μl of H_2O. All reactions were performed in triplicate in 384-well plates as follows: 2 min at 50 °C, 10 min at 95 °C, 40 cycles at 95 °C for 15 s each, and then 60 °C for 60 s using the ABI/Prism 7900HT sequence detector system. The primer sets were designed to span introns and produce a fragment size that would be different from the unspliced product. Ribosomal protein L32 was used as an internal control, and -fold change was calculated using the $2^{-\Delta\Delta Ct}$ method of relative quantification (43). Student's *t* test (two samples assuming equal variances, two-tailed) was used to determine significant differences between control and experimental groups. Primers used for real-time PCR were as follows: Ck1a, 5′-AGCAGCTAGCCAGGATGGAC-3′ (forward) and 5′-CGGTACAGCTTGGCCTCGTA-3′ (reverse); Smr, 5′-AACTGGTCCACCACGCTCAA-3′ (forward) and 5′GGCAACGGAGCATGAACGAA-3′ (reverse); Tis11-1, 5′-AGAATGCAAGTACGGCGAGAAGTG-3′ (forward) and 5′-TGCGGCAGTATTCCGTCTTGTACT-3′ (reverse); Tis11-2 5′-AACCTGCACCGAAAGCTGGA-3′ (forward) and 5′-AAGGTGCGGCAGTATTCCGT-3′ (reverse).

Next Generation Sequencing

Two mRNASeq experiments were performed for this analysis, carried out by the National Institutes of Health Intramural Sequencing Center. In one experiment, 1–5-day-old *w* IE35/BSC5* male flies (referred to below as "null" flies) and w^{1118}*/BSC5* males (referred to as WT or control flies) were collected into separate pools of 40 flies and frozen until use. RNA was isolated from flies using the GE Healthcare RNA isolation kit. The RNA was quantitated using a Qubit fluorometer (Invitrogen). Ten μg of total RNA was transcribed to cDNA and subjected to Illumina deep sequencing analysis using 50-bp paired end reads, generated from an Illumina Genome Analyzer II. There were four separate pools of null and control flies in this experiment.

In a second experiment, 1–5-day-old male *y* w^{67c23} *G1183* flies from the 10-generation backcross and their *y* w^{67c23} controls were used to obtain RNA in the same way and subjected to deep sequencing using 100-bp paired end reads generated from an Illumina HiSeq 2000 system. In this experiment, there were also four separate pools of *G1183* and control flies.

Raw sequence reads were mapped to the cDNA sequences from the *Drosophila* genome using BWA (44), with the default setting of its paired end read mapping protocol. This was done separately for each replicate. The reference cDNA sequences were based on the *Drosophila* genome annotation (version r5.49) from FlyBase. After read mapping, we used the improved version of EpiCenter (45) and the statistical computing language R to perform statistical analyses to identify differentially expressed genes. Specifically, we first filtered out all reads that were not mapped by pairing to the reference cDNA sequences and then counted reads mapping to each cDNA sequence. To quantitate individual transcripts for a "transcript level" analysis, we counted all reads mapped to the entire cDNA sequence of the transcript. For a "gene level" analysis, we counted only reads that were mapped to the common exons shared among all transcript variants from the gene. Read counts of mRNA in each replicate sample were then normalized by the average number of total mapped reads per replicate in both the experimental and control samples. Any transcripts with normalized read counts of less than 100 in both the experimental and control samples were removed from further analysis. For the remaining transcripts, we compared mean expression levels of transcripts that differed significantly between *IE35/BSC5* and *w1118/BSC5* flies, using unpaired, one- or two-tailed Student's *t* tests. Similar comparisons were performed between the mean expression values from the *G1183* flies and their respective controls. In both cases, we also used *p* values adjusted for multiple testing based on EpiCenter's Max-P statistic, which takes into account the total number of tests (45).

NanoString Assays

For confirmation assays, we used the NanoString nCounter method (46) to analyze a subset of the transcripts that were increased in both types of mutant flies as well as two Tis11 transcript variants, Tis11-RA and Tis11-RC, and the CecA1 (Cecropin A1) mRNA. This method uses solution phase

FIGURE 1. **Alignment of *Drosophila* Tis11 with related insect proteins and human TTP family members.** *A*, ClustalW2 alignment of the *Drosophila* Tis11 protein (GenBank™ accession number NP_511141.2) with the corresponding proteins assembled from *Bombyx mori* (XP_004928274) and *Tribolium castaneum* (XP_968440). These two insects were chosen because their predicted protein sequences are the shortest we have found in insects to date. *Asterisks* indicate amino acid identity at that site; *single* and *double dots* indicate weak and strong amino acid similarities, respectively. The residues within the tandem zinc finger domains that are important for zinc coordination are in *red*; the conserved C-terminal domains discussed under "Materials and Methods" in *green*. The *yellow shading* indicates the nuclear export sequence identified in Ref. 48. *B*, ClustalW2 alignment of the *Drosophila* Tis11 protein with the three human TTP family members: TTP (ZFP36) (NP_003398.2), ZFP36L1 (NP_004917.2), and ZFP36L2 (NP_008818.3). *Symbols* and *other markings* are the same as for *A*.

hybridization of RNA to pairs of specific oligonucleotide probes and provides digital quantitation of mRNA levels without amplification. We used the same RNA samples that were used in the mRNASeq analyses, except that only three of the null samples were available.

RESULTS

The D. melanogaster Tis11 Protein—According to current models in FlyBase, the mRNA products of *Tis11* are labeled Tis11-RA, -RC, and -RD. RD is truncated at the extreme 5′-end, but this does not affect the predicted protein sequence. RC has a much longer 3′-UTR than the other two forms but otherwise is identical to Tis11-RA. All three encode the same 436-amino acid protein, which we will refer to as Tis11. An expressed sequence tag clone corresponding to the original A variant was therefore used to make the clones for the transfection and expression studies described here. Although FlyBase and GenBank™ differ somewhat on the isoform nomenclature, the A variant is the same in both databases and is represented by GenBank™ RefSeq numbers NM_078586.4 and NP_511141.2 for the mRNA and protein, respectively.

An alignment of the *Drosophila* Tis11 protein with the shortest insect orthologues we have identified to date, from *Bombyx mori* and *Tribolium castaneum* (253 and 250 amino acids, respectively), is shown in Fig. 1*A*. There is near sequence identity in the TZF domain among the proteins from the three species. There is also a highly conserved region near the extreme C terminus (*green*). The conserved C-terminal region in mammalian ZFP36L1 and ZFP36L2 is known to contain an active nuclear export sequence (7, 47). Recent studies in *Drosophila*

have confirmed that Tis11 is a nucleo-cytoplasmic shuttling protein and have localized the active nuclear export sequence to amino acids 101–113 (Fig. 1*A*, *yellow*) (48). This sequence is not particularly well conserved in the other insects in the alignment shown, but there are neighboring regions of alternating hydrophobic residues that may turn out to be nuclear export sequences. The conserved C-terminal region in human TTP has recently been shown to be responsible for binding to the NOT1 scaffolding protein and appears to be involved in recruiting deadenylases to the protein-RNA complex (33). Outside of these two domains, there was remarkably little sequence conservation between the protein from *D. melanogaster* and those from the other two insects.

We also aligned the *Drosophila* Tis11 protein with the three known human TTP family members: TTP (ZFP36), ZFP36L1, and ZFP36L2 (Fig. 1*B*). A BLAST comparison of the full-length proteins suggests that the Tis11 protein is most closely related to the human ZFP36L1 protein (2E−43), and less closely related to ZFP36L2 (1E−39) and TTP (1E−26). As with the other insects, the predominant regions of conservation are the TZF domain and the extreme C-terminal domain (*green*). The experimentally demonstrated nuclear export sequences in these proteins are *labeled* in *yellow*; note the close overlap between these sequences and the probable NOT1 binding sequences in human ZFP36L1 and ZFP36L2.

For the purposes of this study, in view of the experiments involving C-terminal deletions in Tis11 described below, it is important to note that the conserved C-terminal sequence in *Drosophila* does not appear to contain the nuclear export sequence in this species. In experiments not shown here, we have confirmed the findings by Twyffels *et al.* (48) that *Drosophila* Tis11 is a nucleo-cytoplasmic shuttling protein and that the C-terminal conserved domain does not function as a nuclear export sequence.

Expression of Tis11 in Human Embryonic Kidney 293 Cells—The human embryonic kidney 293 cells (referred to as 293 cells) used in our laboratory are useful for expression studies in this context because they do not express detectable levels of any of the three human TTP family member mRNAs. When the Tis11 protein was expressed in these cells either with (Fig. 2*A*, *lane 2*) or without a His_6 epitope tag (Fig. 2*A*, *lane 3*) and blotted with a Tis11 antibody, both proteins exhibited an apparent M_r of ~55,000–70,000 on SDS gels (Fig. 2*A*). The HA/His_6 epitope-tagged protein migrated at a slightly higher apparent M_r and was approximately as well expressed as the untagged native protein in this transfection system (Fig. 2*A*). No corresponding band was seen in cells transfected with the control vector (BS+, *lane 1*) or on a similar blot incubated with preimmune serum under the same conditions (data not shown). The difference between these values and the predicted size of the untagged protein (M_r 47,166) is probably due to anomalous migration and presumed phosphorylation, as has been seen with the mammalian TTP family members. The possibility of phosphorylation is supported by both the broad band or multiple bands of the immunoreactive protein seen on one-dimensional SDS gels (Fig. 2*A*) and the multiple isoelectric species seen on two dimensional electrophoresis (Fig. 2*B*). This pattern of multiple bands spanning considerable electrophoretic distance has been observed with the mammalian proteins and is thought to reflect multisite phosphorylation (49, 50). The observed two-dimensional gel migration resulted in an approximate isoelectric point of 7.4, which matched well to the predicted pI of 7.4–8.1. Importantly, there was very little apparent proteolysis of the full-length fly protein in this mammalian cell expression system (Fig. 2, *A* and *B*), at least that reacted with the polyclonal antiserum.

The Tis11 protein expressed in 293 cells was then tested for its ability to bind to AU-rich elements (AREs) in mRNAs. As shown in Fig. 2*C*, both the GFP and the HA/His_6 fusion proteins with Tis11 readily bound to RNA probes carrying the ARE sequence derived from the mammalian TTP binding sites in TNF (31) (Fig. 2*C*, *lanes 4* and *7*). Human TTP was used as a positive control (Fig. 2*C*, *lane 2*). To confirm that this binding was due to the presence of the key zinc coordinating residues in the TZF domain, we mutated two of the conserved cysteine or histidine residues within both human TTP and the Tis11 fusion proteins (Fig. 2*C*, *lanes 3*, *5*, *6*, and *8*). Although these mutant proteins were expressed in mammalian cells approximately as well as the wild-type fusion proteins, as determined by Western blotting (Fig. 2, *D* and *E*), they each exhibited essentially no binding to the ARE-containing RNA probes under these conditions (Fig. 2*C*, *lanes 3*, *5*, *6*, and *8*).

Expression of Recombinant Tis11 and RNA Binding—We also expressed the full-length His_6-tagged protein in *E. coli* and purified the resulting expressed protein (Fig. 2*F*, *inset*); this was used in a quantitative binding assay to RNA oligonucleotides using fluorescence anisotropy (Fig. 2*F*). In these experiments, binding of the full-length recombinant fusion protein to a 5′-fluorescein-labeled RNA oligonucleotide based on the mammalian TNF TTP binding site revealed a K_d of 2.3 ± 0.1 nM at 25 °C (n = 2), almost identical to that seen with synthetic peptides derived from the human TTP TZF sequence (8, 35).

When the structure of the Tis11 TZF domain bound to the canonical TTP binding motif UUAUUUAUU was modeled after the solution structure of the human TTP relative ZFP36L2 (TIS11D) (10), a nearly identical predicted structure was produced (Fig. 2*G*). In particular, the aromatic residues Tyr^{152} and Tyr^{190} (yellow), and Phe^{158} and Phe^{196} (green), which are thought to be important for stacking interactions between the aromatic rings and the RNA bases, were identical to those found in the mammalian family members.

Effect of Tis11 on mRNA Stability in HEK 293 Cells—These data demonstrated that full-length Tis11 could bind to RNA ARE sequences with high affinity. However, to address whether Tis11 is an mRNA-destabilizing protein, we first expressed it in 293 cells in the presence of "target" RNAs, containing portions of the mammalian TNF 3′-UTR ARE, that have been validated as sensitive targets of mammalian TTP and its family members (31). We expressed human TTP using the same vector as a positive control. Under these conditions, transfection of low amounts of DNA (5 ng of DNA/plate of cells) of both human TTP (Fig. 3*A*, *lane 2*) and the *Drosophila* Tis11 protein (Fig. 3*A*, *lane 3*) caused decreased accumulation of the target transcript compared with transfection of the vector alone (BS+; Fig. 3*A*, *lane 1*), whereas progressively greater amounts of transfected *Drosophila* Tis11 DNA resulted in a shift of the target transcript

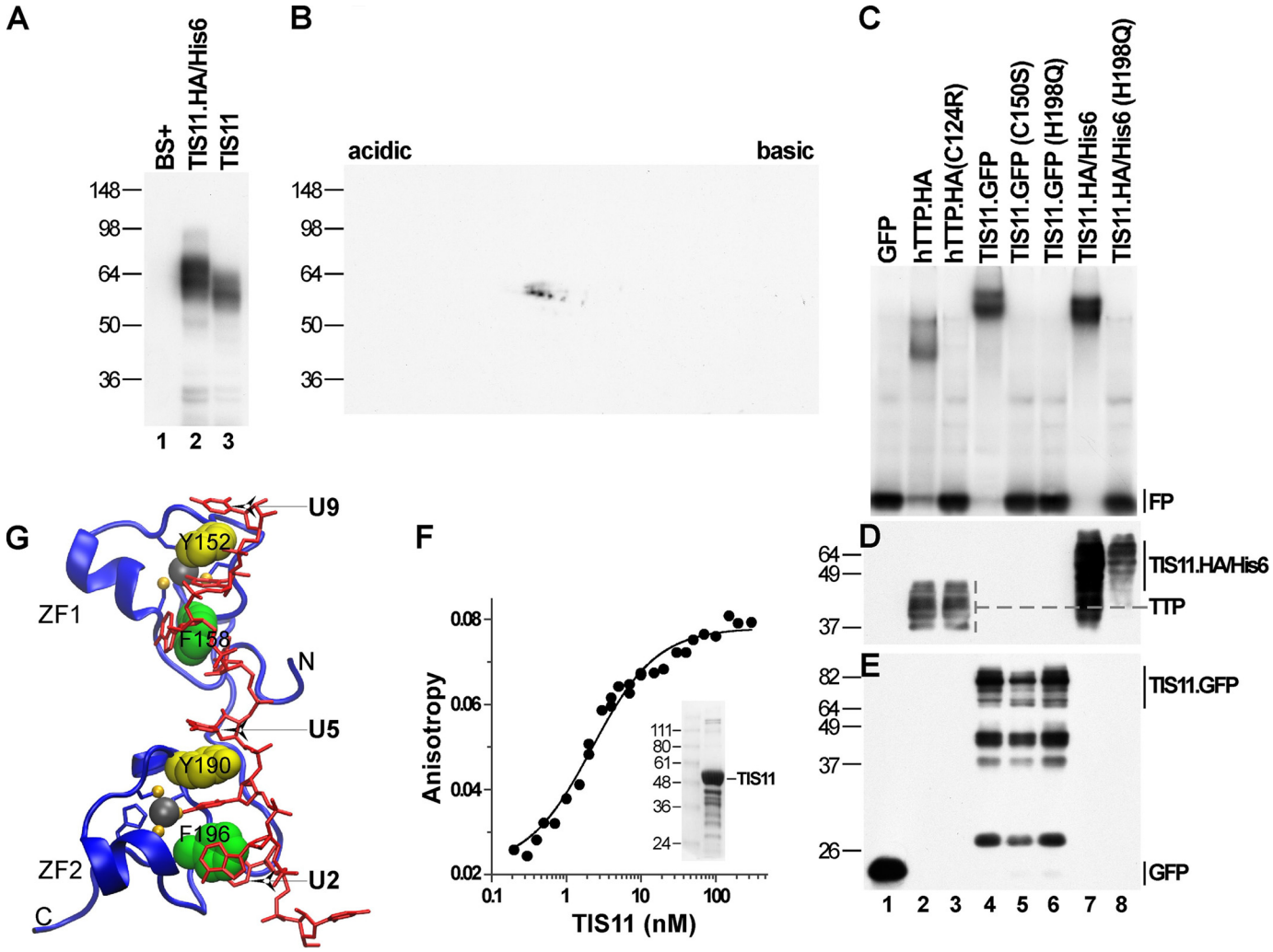

FIGURE 2. **Expression of Tis11 and binding to an ARE-containing RNA probe.** *A* and *B*, Western blots of Tis11 protein expressed in 293 cells blotted with a Tis11 antibody (antibody 1729; 1:5000). In *A*, the blot was from an SDS-polyacrylamide gel. Each *lane* was loaded with 10 μg of cytosolic protein prepared from 293 cells transfected with vector alone (BS+; *lane 1*), Tis11.HA/His6 (*lane 2*), and Tis11 (without an epitope tag; *lane 3*). In *B*, the blot was from a two-dimensional electrophoresis of extract (5 μg) used in *lane 3* in *A*. *C*, autoradiograph of an RNA gel shift experiment using an RNA probe derived from the mouse TNF 3′-UTR. The position of the free probe (*FP*) is indicated. The probes were incubated with 10 μg of cytosolic protein from 293 cells transfected with GFP (*GFP*; *lane 1*) and the same amount of cytosolic protein from 293 cells transfected with plasmids encoding HA-tagged human (*h*) TTP (*lane 2*), the HA-tagged human TTP zinc finger mutant C124R (*lane 3*), the *Drosophila* Tis11-GFP fusion protein (*lane 4*), Tis11-GFP with the first zinc finger mutation C150S (*lane 5*), Tis11-GFP with the second zinc finger mutation H198Q (*lane 6*), the Tis11.HA/His6 fusion protein (*lane 7*), and the Tis11.HA/His6 fusion protein with the second zinc finger mutation H198Q (*lane 8*). *D* and *E*, Western blots (*D* blotted with HA probe (H7)-HRP, sc-7392; *E* blotted with GFP (B2)-HRP, sc-9996, Santa Cruz Biotechnology, Inc.) demonstrating the roughly equivalent expression of the various proteins used for the gel shift experiment in *C*. The positions of the various proteins are indicated to the *right* of *D* and *E*. *F*, analysis of the binding of the purified recombinant protein to an oligonucleotide probe (Fl-AUUUAUUUAUUUA), using fluorescence anisotropy. The average K_d from two similar experiments was 2.3 nM. The *inset* shows a Coomassie Blue-stained gel of the recombinant protein (*second lane*), with molecular weight standards in the *first lane*. *G*, *ribbon diagram* of the simulation solution structure model of the peptide backbone of the Tis11 TZF domain (in *blue*) and *sticks* representing the ARE 9-mer (in *red*). Zinc fingers 1 and 2 (*ZF1* and *ZF2*) and the termini of the peptide (*N* and *C*) are indicated. The side chains of Tyr^{152} and Tyr^{190} (at the CX_5C intervals of finger 1 and finger 2, respectively, in *yellow spheres*) are shown stacking with RNA bases U9-Tyr^{152}-U8 and U5-Tyr^{190}-U4. The side chains of Phe^{158} and Phe^{196} (at the CX_3H intervals of finger 1 and finger 2, respectively, in *green spheres*) are shown stacking with RNA bases A7-Phe^{158}-U6 and A3-Phe^{196}-U2. Also shown are the zinc atoms in *gray spheres* and the side chains of the zinc-coordinating residues of each finger. Nucleosides U9, U5, and U2 are indicated with *arrows*.

to its deadenylated form (*bottom arrow* to the *right* of the *top panel* in Fig. 3*A*), which then accumulated to an even greater extent at higher levels of transfected Tis11 DNA. This paradoxical increase in the apparently deadenylated target transcript at higher concentrations of transfected DNA has previously been seen with other TTP family members in this assay (31, 51). Surprisingly, transfection of the same low amount of the human TTP DNA plasmid (Fig. 3*A*, *lane 2*) caused approximately the same extent of transcript depletion as Tis11 (Fig. 3*A*, *lane 3*), not only indicating that the *Drosophila* protein was effective at promoting transcript decay in this experimental system but suggesting that it was active at roughly the same concentrations as human TTP. Fig. 3, *B* and *C*, demonstrates the expression of both TTP and Tis11 mRNAs in this experiment.

To confirm that the lower band seen after TTP or Tis11 expression was the deadenylated form of the target transcript, we performed RNase H/oligo(dT) incubations with the RNA samples shown in Fig. 3*A*, as described previously (41). Fig. 3*D* shows a Northern blot, using a TNF cDNA probe, of the RNA samples shown in Fig. 3*A*, both before and after treatment with RNase H. As shown in the *pair* of *lanes labeled 1*, using an RNA sample from the original *lane 1* in Fig. 3*A*, RNase/

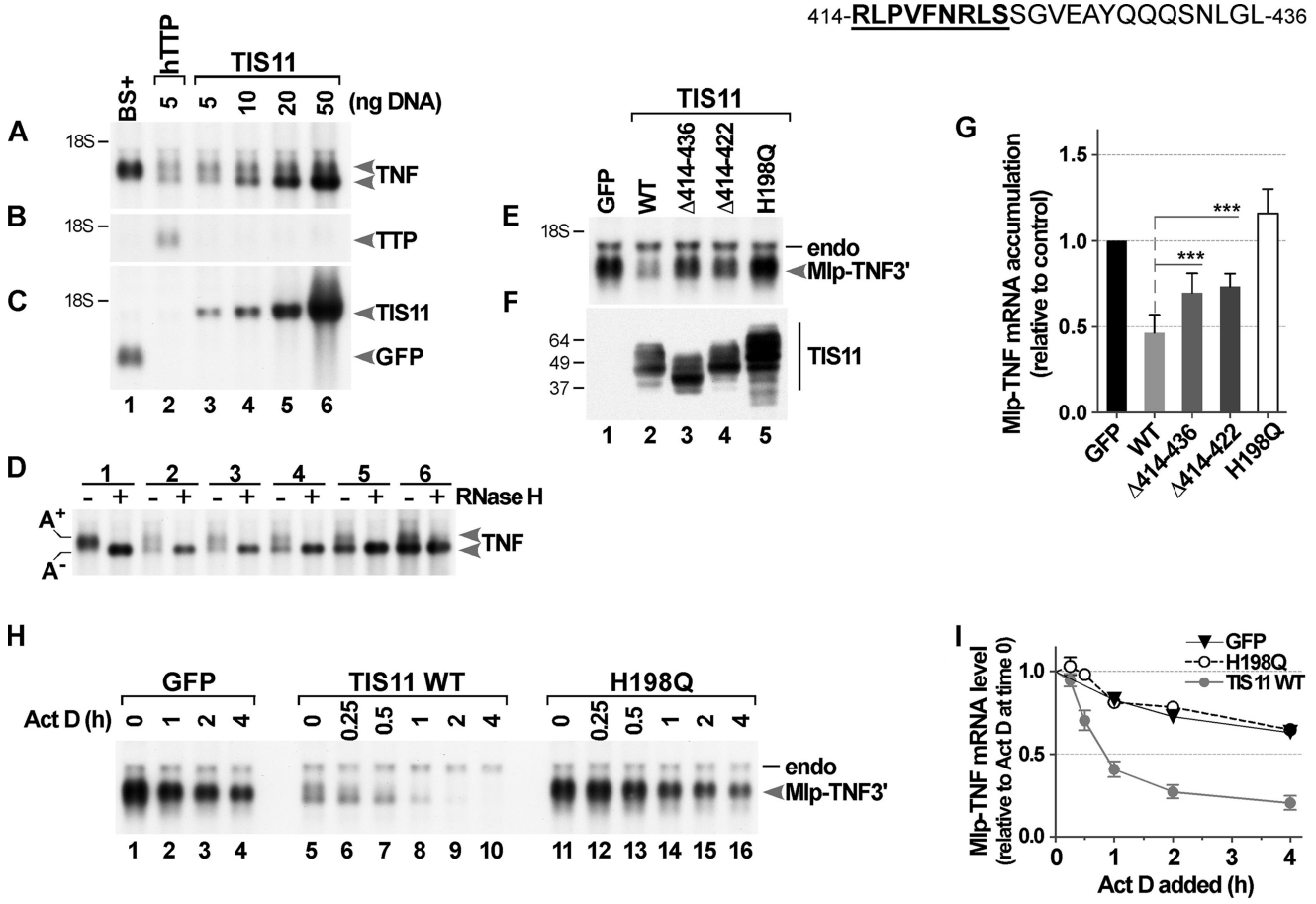

FIGURE 3. **Tis11-promoted mRNA decay and deadenylation.** *A*, Northern blot demonstrating the effect of Tis11 to promote the decay of mouse TNF mRNA. *A* shows the level of TNF mRNA accumulation after co-transfection of a TNF plasmid (CMV.mTNFα) (31) with the vector BS+ (*lane 1*), 5 ng of a construct encoding human TTP (CMV.hTTP.tag; *lane 2*), and a 10-fold range of amounts of a construct encoding Tis11 (CMV.DTis11.HA/His_6; *lanes 3–6*). The *two arrowheads labeled TNF* indicate the fully adenylated (*top arrowhead*) and deadenylated (*bottom arrowhead*) TNF mRNA. *B*, a similar blot that had been probed with a TTP cDNA; *C*, a similar blot that had been probed with a mixture of Tis11 and GFP cDNAs, documenting the expression of Tis11 mRNA at the different amounts of transfected DNA. At 5 ng of transfected human TTP DNA (*A*, *lane 2*), there was a marked decrease in TNF mRNA accumulation compared with control (*A*, *lane 1*); this was accompanied by the appearance of a lower, presumably deadenylated band of TNF mRNA. When Tis11 DNA was transfected at the same low concentration (5 ng; *A*, *lane 3*), there were a decrease in TNF mRNA accumulation and the appearance of a lower mRNA band that were similar to the accumulation seen with 5 ng of transfected human TTP DNA. At 10 ng of *Tis11* plasmid (*A*, *lane 4*), there was still a decrease in total TNF mRNA accumulation compared with the control transfection, but there was increased accumulation of the lower, deadenylated band of the TNF transcript. With increasing amounts of transfected Tis11 DNA above 10 ng, there was an increase in the accumulation of the deadenylated form of the TNF mRNA (*A*, *lanes 5* and *6*, indicated by the *bottom TNF arrow*). See the Western blots shown in Fig. 2*D* for protein expression from 293 cells transfected with the same constructs expressing human TTP (*lane 2* of Fig. 2*D*) or Tis11 (*lane 7* of Fig. 2*D*). *D*, results of an RNase H/oligo(dT) experiment, with the *pairs of lanes numbered 1–6* representing the samples from those lane numbers in *A*. The presence or absence of RNase H is indicated by the *plus* and *minus signs*. RNA from these incubations was subjected to Northern blotting with a TNF cDNA probe. The *band labeled* A^+ indicates the fully polyadenylated form of the transfected expressed mRNA, and the *band labeled* A^- indicates the deadenylated form of this transcript. In the *top right-hand corner* of the figure is shown the sequence of the Tis11 protein C terminus, from residue 414 to the C terminus (of NP_511141), with Arg^{414}–Ser^{422} *underlined*. *E*, representative Northern blot demonstrating the involvement of the Tis11 C-terminal domain to promote the decay of a fusion Mlp-Tnf3′ mRNA. The *top band* seen in each lane (*endo*) shows the level of endogenous MLP mRNA that served as a loading control for subsequent calculations. The *lower band* shows the levels of the fusion Mlp-Tnf3′ mRNA accumulation after co-transfection of the Mlp-Tnf3′ plasmid (3 μg/plate) with EGFP (5 ng/plate, *lane 1*), a construct encoding WT HA.Tis11 (*lane 2*), or constructs encoding mutants of HA.Tis11 (amino acids 414–436 deleted (*Δ414-end*, *lanes 3*), amino acids 414–422 deleted (*Δ414–422*, *lanes 4*) or the construct Tis11.HA/His_6(H198Q), in which the zinc-coordinating His^{198} in finger 2 was mutated to Gln (*H198Q*; *lanes 5*). The constructs expressing Tis11 were co-transfected at 10 ng/plate. *F*, Western blot of protein extracts prepared from 293 cells transfected with the same constructs expressing Tis11 or its deletion or zinc finger mutants, as indicated. Each plate of cells was transfected with 0.2 μg of expression construct DNA, together with 4.8 μg of vector BS+ DNA. Each *gel lane* was loaded with 10 μg of extract protein, and an antibody directed at the HA epitope was used for blotting. *G*, comparison of the effects of mutant and WT Tis11 on the accumulation of the Mlp-Tnf3′ mRNA, expressed relative to control (EGFP co-transfection as control, mean ± S.D. (*error bars*)) from the results of six similar co-transfection assays. Each of the Northern blots was quantitated using a PhosphorImager, and the level of Mlp-Tnf3′ mRNA expression of each gel lane was normalized to the endogenous Mlp mRNA expression level. To compare the effects between mutant and WT Tis11 on the accumulation of the Mlp-Tnf3′ mRNA, two-tailed Student's *t* tests were performed, as indicated by the *dotted line* (***, $p < 0.001$), with a Bonferroni correction applied when needed for multiple comparisons. In *H*, 293 cells were co-transfected with constructs expressing either GFP, WT Tis11, or the mutant Tis11 H198Q, along with a construct encoding an Mlp-Tnf3′ fusion mRNA, as described in detail under "Materials and Methods." Total cellular RNA was prepared from three plates of cells for each condition and was used for Northern blots, hybridized with a mouse Mlp cDNA. The *arrows* point to bands corresponding to endogenous 293 cell MLP mRNA (*endo*) and the transfected-expressed Mlp-Tnf3′ mRNA. In *I*, results were averaged from five experiments that were identical to that shown in *H*, and the mean values from these experiments ± S.D. were plotted as fractions of the values at time 0. These values were based on PhosphorImager quantitation of the Mlp-Tnf3′ mRNA, normalized for endogenous Mlp mRNA. The *dashed lines* indicate 100 and 50% of the original value.

oligo(dT) treatment caused a decrease in the size of the hybridizing TNF mRNA band, representing a change from the polyadenylated transcript (A^+) to the deadenylated transcript (A^-) (Fig. 3*D*). The *lower bands* seen after both TTP and Tis11 expression migrated to an identical position as the deadenylated bands in every case (*pairs* of *lanes 2–6* in Fig.

3*D*), supporting their identification as deadenylated forms of the TNF transcript.

These data established that Tis11 is an ARE-binding and mRNA-destabilizing protein that can behave the same way as the mammalian TTP family proteins to decrease the levels of, and apparently deadenylate, target mRNAs in this co-transfection assay in a heterologous mammalian cell system.

These results suggested that conserved sequence domains between the fly and mammalian proteins might be involved in, for example, recruiting deadenylase complexes to the Tis11 bound to mRNA. Because the only apparently conserved sequences outside of the TZF domain were in the extreme C terminus (see Fig. 1*B*), we deleted this conserved domain in the untagged *Drosophila* protein and examined the effects of these deletions on Tis11 activity in the 293 cell co-transfection system. Based on similar analyses done with the human TTP protein (33), we hypothesized that the conserved C-terminal motif would be important for the mRNA-degrading activity of Tis11, possibly by recruiting a similar Not1 complex. The sequence of the C-terminal end of the Tis11 protein, from residue 414 to the end, is shown in the *top right-hand corner* of Fig. 3; *underlined* in *boldface type* are the residues of the putative Not1 binding sequence discussed below.

As shown in Fig. 3*E*, using a mouse Mlp mRNA protein coding domain fused to a portion of the mouse Tnf mRNA as a target transcript (33), the N-terminal HA-tagged *Drosophila* Tis11 protein was effective in decreasing the steady-state levels of the target transcript (Fig. 3*E*, compare *lanes 1* and *2*). On average, this decrease was ~53.5 ± 10% under these conditions ($p < 0.0001$, using a two-tailed *t* test) (Fig. 3*G*). When the last 23 amino acids of the C terminus (Arg^{414}–Leu^{436}) were removed or when the nine amino acids (Arg^{414}–Ser^{422}) that comprise the conserved putative Not1 binding domain were removed by an internal deletion, the protein was less effective at promoting mRNA decay than the WT protein (target transcript decreased by 30.2 ± 11.4 and 26.5 ± 7.5%, respectively) (Fig. 3, *E* (*lanes 3* and *4*) and *G*). When the effectiveness in promoting mRNA decay was compared, both of these deletion mutants were significantly less effective than the WT protein (one-way analysis of variance, Tukey's multiple comparison test; Fig. 3*G*). However, there was no significant difference between these two mutants, suggesting that the 14 amino acids (Ser^{423}–Leu^{436}) immediately C-terminal of the conserved domain were not critical for the induced mRNA decay. As expected, when the non-binding zinc finger mutant H198Q protein was co-expressed with the target transcript, there was no effect on steady state levels of the target mRNA compared with EGFP alone (no Tis11) (Fig. 3*E*, compare *lanes 1* and *5*; also see Fig. 3*G*). The mutant proteins were expressed in these experiments at comparable levels (Fig. 3*F*).

To examine the effect of WT Tis11 on mRNA decay, we performed separate co-transfection experiments and examined the time course of decay of the Mlp-Tnf3′ fusion mRNA decay in the presence of WT Tis11 or one of its non-binding mutants (Fig. 3*H*). This construct uses the mouse *Mlp* promoter to drive the expression of a fusion transcript comprising mouse Mlp mRNA and a portion of the mouse Tnf mRNA (33); this promoter is inhibited by actinomycin D, in contrast to the CMV promoter used elsewhere. Each plate of 293 cells was co-transfected with 3 μg of the Mlp-Tnf3′ target plasmid and 2 μg of vector (BS+) DNA and, as noted in the figure, 5 ng of a EGFP construct with 5 ng of CMV/BS+ vector DNA (GFP), 10 ng of CMV.DTis11.HA/His6 (TIS11 WT), or 10 ng of the TIS11 construct containing the H198Q mutation (H198Q). Twenty-four hours after removing the transfection mixture, actinomycin D (5 μg/ml) was added to each plate, and samples were prepared at the indicated times for RNA preparation. Each sample represents RNA from three plates of cells. A representative Northern blot from these experiments was probed with a mouse Mlp cDNA probe (Fig. 3*H*); the band labeled *endo* refers to endogenous human MLP mRNA, and the band labeled *Mlp-Tnf3′* indicates the fusion target mRNA. Under these conditions, the transfected Mlp-TNF3′ mRNA was reasonably stable for 4 h after the actinomycin D addition in the GFP-transfected cells (Fig. 3*H*, *left*). When WT Tis11 was expressed, there was a marked decrease in the steady state levels of the transfected-expressed Mlp-Tnf3′ mRNA as well as an apparent rapid disappearance of this transcript with time, with perhaps slower disappearance of the lower, deadenylated form of the transcript (Fig. 3*H*, *middle*). In contrast, the co-transfection of the H198Q mutant Tis11 protein did not affect either the steady state levels of target mRNA before actinomycin D treatment or the apparent decay of the target mRNA after actinomycin D (Fig. 3*H*, *right*). Endogenous levels of human MLP mRNA did not change markedly during these manipulations and served as an internal loading control. We also performed RNase H-oligo(dT) assays on the samples from this experiment taken from the cells before the actinomycin D treatment and found migration patterns of the polyadenylated and deadenylated mRNA species that were similar to those shown in Fig. 3*D* (data not shown).

Northern blotting data from five such experiments were quantitated using a PhosphorImager and were averaged in Fig. 3*I*, with the steady state levels before actinomycin D normalized to 1.0 at 0 h. Means ± S.D. were plotted in this figure. When either GFP or the H198Q mutant of Tis11 was co-transfected, the decay lines were superimposable and decreased to ~70% of time 0 after 4 h. In contrast, the target transcript decayed rapidly in the Tis11-transfected cells, reaching 50% of the original level after 50 min. These data support the concept that Tis11 promoted the decay of this ARE-containing transcript in a manner that is completely dependent on the integrity of the TZF domain.

Structural Models of the Drosophila Tis11 Putative Not1 Binding Domain—To explore further the feasibility of the Tis11 C-terminal domain as a Not1 binding domain, we performed simulation solution modeling of the proposed association between the Tis11 C-terminal peptide and the putative *Drosophila* Not1 Tis11 binding domain, based on the original coordinates of Fabian *et al.* (33). The C-terminal sequences from human TTP and *Drosophila* Tis11 are aligned in Fig. 4*A*, with the demonstrated human NOT1 and putative *Drosophila* Not1 binding domains in *boldface type*; the *symbols* are described in the legend to Fig. 1. Fig. 4*B* shows the proposed structures of the binding complex formed by either the human TTP C-terminal peptide (*red*) or the *Drosophila* Tis11 C-terminal peptide

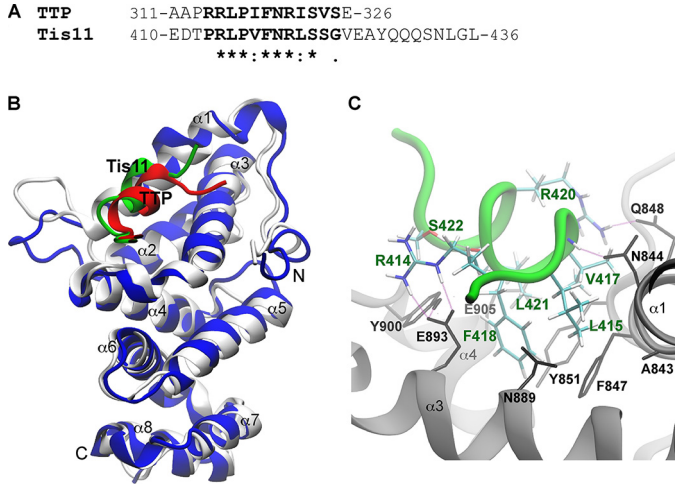

FIGURE 4. **Simulation solution structures of the human and *Drosophila* NOT1 peptides binding to the human TTP and *Drosophila* Tis11 C-terminal peptides.** *A*, sequences and numbering of the aligned C-terminal regions from human TTP and *Drosophila* Tis11, as shown in Fig. 1*B*. *Asterisks* and *other symbols* are as described in the legend to Fig. 1. In *B*, the *ribbon diagram* shows the backbone superposition of human NOT1 (*silver*; residues 820–999 of GenBank™ accession number NP_001252541.1), *Drosophila* Not1 (*blue*; residues 892–1071 from NP_001097242.1), and C-terminal peptides of human TTP (*red*; residues 315–325 of GenBank™ accession number AAH09693.1) and *Drosophila* Tis11 (*green*, residues 413–424 of NP_511141). *C*, a *ribbon diagram* of the proposed interface between the TTP binding domain of the human NOT1 protein (*silver*) and the Tis11 C-terminal peptide (*green*). Interacting side chains of NOT1 (*gray*) and Tis11 peptide (*colors*, with *green labels*) are shown as *sticks*. Hydrophobic interactions that are thought to strengthen the interaction are shown between the side chains of NOT1 (Phe^{847}, Tyr^{851}, Tyr^{900}, hydrophobic portions of Asn^{889} and Glu^{905}) and Tis11 (Leu^{415}, Val^{417}, Phe^{418}, and Leu^{421}). Note that the salt bridges formed between the side chains (NOT1 Glu^{893} and Arg^{414} of Tis11, 2.75 and 2.85 Å; NOT1 Gln^{848} and Arg^{420} of Tis11, 2.80 Å) and hydrogen bonds (Glu^{893} and Tyr^{900} of NOT1; NOT1 Asn^{844} and Val^{417} backbone of Tis11, 2.81 Å; and backbones of Tis11 Phe^{418} and Ser^{422}) also contribute to the predicted stability of the interface. The predicted bonds formed are shown in *magenta*.

(*green*) to the TTP binding domain of human NOT1 (*silver*) and *Drosophila* Not1 (*blue*), demonstrating that the proposed *Drosophila* complex is structurally very similar to the complex formed between the two human proteins (33). In fact, essentially all of the key residues in the human protein complex are present in the putative *Drosophila* protein complex (Fig. 4*B*). In Fig. 4*C*, we also modeled the proposed interaction between the *Drosophila* Tis11 C-terminal peptide shown in A (*green*) with the human NOT1 TTP binding site (*silver*). The potentially interacting side chains of NOT1 (*gray*) and the Tis11 peptide (*colors*, with *green labels*) are shown as *sticks*. Hydrophobic interactions, salt bridges, and hydrogen bonds, shown in *magenta*, presumably contribute to the predicted stability of the interface (Fig. 4*C*).

These data suggest that the conserved C-terminal domain in *Drosophila* is likely to serve as the binding site for either the human or *Drosophila* Not1 protein, which in turn can serve as the scaffolding for the entire CCR4-NOT1 deadenylating complex. As with the human TTP protein (33), deletion of the presumed Not1 binding domain of Tis11 does not totally abrogate its mRNA-degrading activity, suggesting that other binding sites for other mRNA-degrading activities may exist in both proteins. Importantly, the deletions that impaired mRNA deadenylating activity had no effect on nucleoplasmic shuttling (data not shown; also see above), excluding this as a potential artifact in the interpretation of these experiments.

Loss of Function Experiments in Adult Male Flies—Tis11 is on the *Drosophila* X chromosome, and Fig. 5*A* shows a diagrammatic representation of this locus and neighboring loci (*Ck1α* and *Smr*), with the centromere to the *right*. The two *EP* elements discussed in this paper are shown at the *top*, with the *vertical dotted lines* indicating their position in the first exon of *Tis11* and ultimately in the 5′-UTR of the Tis11 mRNA, as well as their directions of transcription. The approximate locations of the *IE35* imprecise excision and the *BSC5* duplication are also indicated. Transcription of *Tis11* occurs from *left* to *right* in this figure. Note the *broken lines*, indicating the removal of 15 kb from the large second intron of *Tis11*.

To begin to explore the possible function of Tis11 in intact flies, we conducted an imprecise excision screen by mobilizing the *P* element in *G147* flies, and chromosomes were screened over *Df(1)N105*. In this screen, lethality was used to identify imprecise excision, because, given the lethality seen in the initial *G1183* stock obtained from GenExel, we assumed that a *Tis11* deficiency would have a lethal phenotype. All 45 of the lethal chromosomes recovered were also deficient for one of the neighboring genes, *Ck1α* or *Smr*. One of the imprecise excision events, *Df(1)Tis11-IE35*, was balanced over *FM7i*, *Act5C-GFP*. The *IE35* hemizygous males died at the first or second larval instar. To map the extent of the *IE35* deficiency, first instar larvae were used for the purification of genomic DNA and analyzed by PCR. This analysis confirmed that *IE35* was deficient in both *Tis11* and *Smr*. Real-time RT-PCR of *IE35* males carrying *Dp(1;Y)BSC5*, a Y chromosome with a duplication of a portion of the X chromosome containing *Smr*, demonstrated the absence of Tis11 transcripts, whereas CK1a and Smr transcript levels were not affected (Fig. 5*B*). Further PCR analyses showed that *IE35* is a deletion of ~200 kb that extends from the first exon of *Tis11*, where the original *P* element was inserted, proximally to *CG4661*. Analysis of *Dp(1;Y)BSC5*, using genomic PCR from *IE35/BSC5* and w^{1118}/*BSC5* males, indicated that the 5′-end of the X chromosome fragment of the *BSC5* duplication appears to be in the 3′-flanking region between *Tis11* and *Smr*, because PCR products were not detected 1.8 kb downstream from the 3′-end of *Tis11* mRNA but were detected in the last exon of *Smr*. Therefore, *IE35/BSC5* males carry all of the genes lost in *IE35* except for *Tis11*. These males will be referred to as *Tis11* "null" flies. *Tis11* null males were viable and fertile and appeared normal, although they exhibited a modest (~24-h) delay in eclosion (data not shown). Given the extents of *IE35* and *BSC5*, these males also carry two copies of ~13 genes distal to *CG32650*[6] (also see below).

We also used *G1183* flies as a completely separate genotype that might lead to Tis11 depletion, presumably by the *EP* element interfering with transcription from the first exon. As described under "Materials and Methods," this mutation was initially lethal when it arrived in the laboratory but spontaneously reverted to a viable phenotype after several months of propagation (*G1183v*). We also generated a viable stock

[6] K. Cook and E. Spana, personal communication.

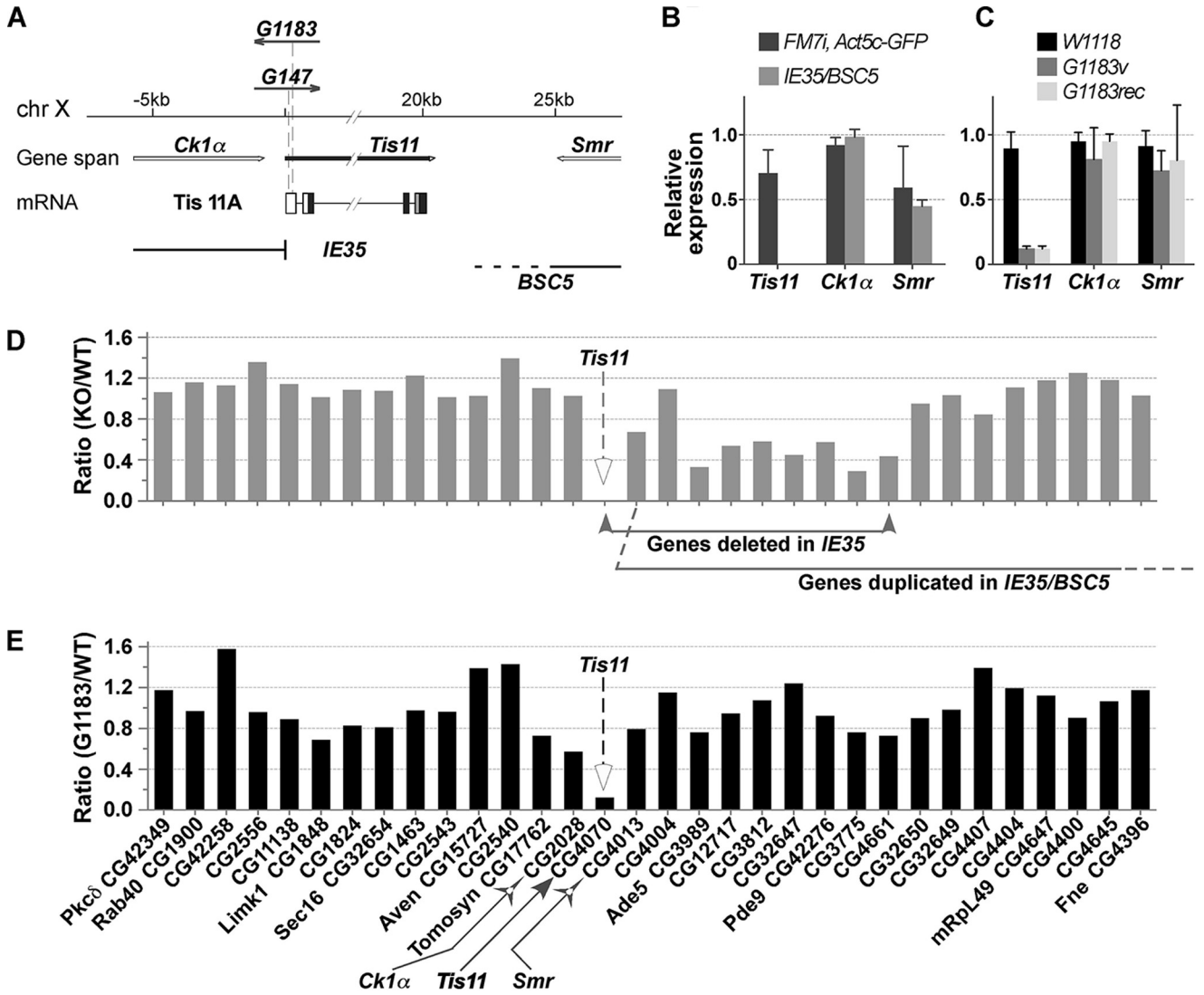

FIGURE 5. **The *Tis11* locus and transcript expression in the two types of mutant flies.** *A*, a portion of the *Drosophila* X chromosome, comprising the *Tis11* locus and neighboring genes, with the centromere to the *right*. The positions of the *P{EP}G1183* and *P{EP}G147* transposons within the first exon of *Tis11* are indicated by the *vertical dashed lines*; the *arrows* indicate the direction of transcription driven by UAS promoter elements within the transposons. *IE35* is an imprecise excision allele obtained by mobilizing the *P{EP}G147* transposon. It deletes *Tis11* from the *P* element insertion site and extends into the neighboring *Smr* locus. *Dp(1;Y)BSC5* is a Y chromosome bearing an X chromosome fragment that contains *Smr* but not *Tis11*. The combination of *IE35* and *BSC5* results in a complete loss of *Tis11* expression but normal *Smr* expression. *Dotted portions of the line* reflect an uncertain end point. The positions and transcription directionality of the *Ck1α* and *Smr* loci are shown. The exons comprising the Tis11 mRNA are indicated, with *no shading* representing the 5′-UTR, and *light gray shading* representing the TZF domain of the protein. The *broken line* indicates a large gap in the locus representing ~15 kb of intron 2. Shown in *B* are real-time RT-PCR data, showing means ± S.D. (*error bars*), from *IE35* males carrying *Dp(1;Y)BSC5*, a Y chromosome with a duplication of *Smr*, demonstrating the absence of Tis11 transcripts in the null flies, whereas CK1α and Smr transcript levels were not affected. In *B*, transcript levels were measured from 1–5-day-old *IE35/BSC5* males compared with *FM7i*, *Act5C-GFP/BSC5* sibling males of the same age. Five pools of 30 flies each were collected for each stock. *C*, similar real-time RT-PCR data from WT flies and two types of *G1183* flies, viable flies that spontaneously arose from the original lethal stock (*G1183v*), and viable flies that were intentionally recombined to remove lethal mutations elsewhere, as discussed under "Materials and Methods" (*G1183rec*). For the analysis shown in *C*, *G1183v*, *G1183rec*, and w^{1118} 0–1-day-old males were frozen and collected into three pools each of 25–40 flies in each pool. The RNA samples used for *B* and *C* were different from the samples used for the mRNASeq analysis discussed below. The adult male *G1183* flies of both types expressed approximately one-eighth of the normal level of Tis11 mRNA (*C*), but *Smr* and *Ck1α* expression were unaffected in either the spontaneous (*G1183v*) or recombinant (*G1183rec*) flies. In *D* and *E* are shown gene level ratios of transcript expression from the mRNASeq experiments for the genes around *Tis11* on the *Drosophila* X chromosome, with *D* showing the ratios of null/control and *E* showing the ratios of *G1183*/control (the centromere is to the *right* in both *panels*). In *D*, the location of genes deleted in *IE35* and the genes duplicated in *BSC5* are indicated at the *bottom* of the *graph*. Note the absence of Tis11 transcript expression in *D* as well as the depressed expression of several genes centromeric to *Tis11* on the X chromosome. In *E*, the Tis11 transcripts were decreased by 8.6-fold, but most neighboring genes were relatively unaffected in the *G1183* flies.

(*G1183rec*) by allowing meiotic recombination with w^{1118}, as discussed under "Materials and Methods." The adult males of both *G1183v* and *G1183rec* were viable and fertile and expressed approximately one-eighth of the normal level of Tis11 mRNA (Fig. 5*C*); these alleles can therefore be viewed as stable hypomorphic alleles of *Tis11*. As shown in Fig. 5*C*, neither *Smr* nor *Ck1α* expression was affected in either the spontaneous (*G1183v*) or recombinant (*G1183rec*) flies. We then back-crossed the *G1183rec* flies into the $y\ w^{67c23}$ background for 10 generations for the mRNASeq data experiments performed for this paper. As before, these flies were viable and fertile, although they also exhibited eclosion delays of ~24 h.

Deep Sequencing—Our working hypothesis was that depletion of Tis11 should lead to the abnormal accumulation of one or more of its target mRNAs. To search for potential target transcripts for Tis11 in adult flies, we first performed deep sequencing of transcripts (mRNASeq) on poly(A)$^+$-selected RNAs from null males. Values were compared with those obtained from w^{1118}/*BSC5* controls. We also performed a similar experiment with the *G1183* males and their respective controls and compared these results with the results of the experiment with the null flies. The complete data set from these comparisons has been deposited in the Gene Expression Omnibus (accession number GSE58937).

Because the combined deletion/duplication approach for knocking out *Tis11* was likely to lead to alterations in the expression of neighboring genes through the phenomenon of position-effect variegation (52), we evaluated levels of expression for the genes flanking *Tis11* on the X chromosome. For this purpose, we used the read counts from the shared exons from all of the transcript variants for a given gene (*i.e.* a gene level comparison). We plotted these as the ratios of null/control average expression levels (Fig. 5*D*). We performed a similar analysis with the *G1183 versus* control experiment (Fig. 5*E*). In the *Tis11* null flies, expression levels of the transcripts expressed by genes on the *X* chromosome that were distal (*i.e.* telomeric from) *Tis11* were remarkably normal (Fig. 5*D*). As expected, Tis11 mRNA was not detected in the null flies. However, as predicted from the position-effect variegation concept (52), several genes close to *Tis11* exhibited decreased expression in the null flies compared with controls; further away from the *Tis11* locus, expression levels in the null flies returned to normal (Fig. 5*D*). We performed a similar analysis on the ratios of the average read counts for the *G1183* flies compared with control (Fig. 5*E*). Other than Tis11 mRNA, which was down-regulated by ~8.6-fold in these flies, the only significant change noted was a modest (~40%) decrease in the expression of the immediately telomeric gene, *Ck1α*, in the *G1183* flies.

We next identified transcripts at the individual transcript variant level that were increased by 1.5-fold or more in both the *Tis11* null flies and the *G1183* flies, with $p < 0.05$ using unpaired Student's *t* tests. We identified 379 transcripts that were elevated in the null flies compared with controls using these criteria. In the *G1183* experiment, there were 1430 up-regulated transcripts, using the same criteria. When we compared the two data sets, we identified 69 transcripts, representing 56 genes, that were elevated in both experiments by at least 1.5-fold with $p < 0.05$. Table 1 shows the transcripts that were increased according to these criteria, along with their -fold increases in the Tis11-deficient flies compared with controls and the *p* and *q* values. We also searched the relevant 3′-UTRs from FlyBase for the presence of the core 5-mers for TTP family protein binding sites (AUUUA) as well as the longer 7-mer core binding site (UAUUUAU). Of the 69 transcripts, 34 (49%) contained at least one binding site 7-mer, whereas many more contained at least one core 5-mer. This compares with a frequency of 7-mers in the 3′-UTRs of *Drosophila* expressed transcripts of ~27% (data not shown); the difference between the two frequencies was significant by the hypergeometric test at 1.8E−05. Finally, we searched FlyBase for predicted cellular functions for each of the elevated genes (Table 1). A wide variety of potential functional classes of proteins was represented, but the most common cellular function listed as the primary functional term was proteolysis, listed as a primary defining term for 10 of the 69 jointly elevated transcripts.

A subset of the transcripts listed in Table 1 as well as some of the Tis11 isoforms were analyzed by NanoString nCounter analysis (46), using many of the original RNA samples used in the mRNASeq analyses. Only three of four of the null samples were available for this analysis. Of 42 up-regulated transcripts from Table 1 that were analyzed by this means, one was removed because the assay yielded results that were below the upper limit of the negative controls. Of the 41 remaining transcripts, eight were not significantly increased in either comparison, 12 were significantly up-regulated ($p < 0.05$ using unpaired, two-tailed Student's *t* tests) in one comparison, and 21 were significantly up-regulated in both types of mutant flies. The results from these confirmation assays are indicated by *asterisks* in Table 1, and a subset is shown graphically in Fig. 6 (see below).

As determined by mRNASeq analysis, there was no detectable expression of Tis11-RC, the longest transcript variant for *Tis11*, in the null flies, and this transcript was decreased 8.6-fold in the *G1183* flies (Fig. 6*A*, *left*). Very similar changes in transcript levels were observed in the NanoString confirmation assays (Fig. 6*A*, *right*). In Fig. 6*B*, each *panel* represents the average depth of read coverage from the four biological samples used for each set, covering the 5′-end of the Tis11-RC mRNA. The *arrow* points to the site of insertion of the *G1183 EP* element. There were no detectable transcript reads 5′ of the site of *EP* element insertion (Fig. 6*B*). Note that the *vertical axis* in the *fourth panel* (*G1183*) is 10-fold expanded compared with the other three. Shown in Fig. 6, *C* and *E*, are the means ± S.D. of the expression results from two ect transcript variants, ect-RA and ect-RD, which have different 3′-UTRs. In both cases, these results were confirmed by the NanoString assays (*right panels* in Fig. 6, *C* and *E*. The alignments in Fig. 6, *D* and *F*, show sequences from the ect-RA and ect-RD transcripts compared with orthologous sequences from other *Drosophila* species contained in the "classical" tree, with the optimum binding heptamer UAUUUAU *highlighted* in *red*. Identical residues at each position are indicated by *asterisks*. In Fig. 6*G* are shown the transcript expression results for the mRNA encoding Rab18, a small GTPase, whose 3′-UTR contains only a single heptamer binding site that is less well conserved in some of the evolutionarily more distant *Drosophila* species (Fig. 6*H*). The increases in both mutants were confirmed by NanoString assays (of Fig. 6*G*, *right*). In Fig. 6, *A*, *C*, *E*, and *G*, all differences between the respective pairs of means were significant ($p < 0.01$).

We performed a similar analysis for the down-regulated transcripts. In the experiment comparing the null flies with controls, 623 transcripts were down-regulated more than 1.5-fold with $p < 0.05$. In the experiment comparing *G1183* flies with controls, 568 transcripts met the same criteria. When the data from the two experiments were combined, there were only 26 transcripts, representing 19 genes, in common between the two lists of mRNAs that were down-regulated by 1.5-fold or

TABLE 1

Transcripts up-regulated in adult *Tis11* null and hypomorphic males

The data shown here are from the two mRNASeq experiments described under "Materials and Methods." For the column labeled "KO/Control," the results are expressed as -fold changes of transcript levels in the *IE35/BSC5* "null" males divided by transcript levels in the w^{1118}/*BSC5* males used as controls. For the column labeled "*G1183*/Control," the results are expressed as -fold changes in transcript levels in the *G1183* males over the $y\ w^{67c23}$ males used as controls. In each case, the Max-P and *t* test *p* values of the comparisons of the means from experimental *versus* control are shown. The column labeled "5-mers" shows the number of core 5-mers from the optimum TTP family member binding site, AUUUA, in the FlyBase annotated 3′-UTRs for each transcript; similarly, the column labeled "7-mers" shows the number of 7-mers, UAUUUAU, in the FlyBase annotated 3′-UTRs. The final column refers to the Gene Ontology molecular function or biological process from FlyBase; blanks indicate that no function or process was listed for that transcript. In the column "Gene name," a double asterisk indicates that both comparisons were statistically significant and in the same direction in the NanoString assay, and a single asterisk indicates that one of the two comparisons was significant; NC indicates "not confirmed" in either comparison; and a blank indicates that that transcript was not checked in the NanoString assay.

GeneAcc	Gene name	KO/ control	Max-P *p* value	*t* test *p* value	G1183/ control	Max-P *p* value	*t* test *p* value	5-mers	7-mers	GO molecular function or biological process
FBtr0071845	babos-RA*	1.57	4.17E−01	1.07E−03	1.72	1.81E−02	3.41E−06	1	1	Dendrite morphogenesis?
FBtr0339539	babos-RB	1.53	5.07E−01	4.30E−04	1.81	8.40E−03	7.13E−07	1	1	Dendrite morphogenesis?
FBtr0071690	CG10433-RA**	1.86	6.66E−02	1.52E−05	2.22	1.17E−04	2.79E−08	2	1	
FBtr0071691	CG10433-RB	1.77	1.18E−01	1.52E−04	2.17	2.12E−04	3.59E−07	2	1	
FBtr0089630	CG10910-RB	1.65	1.00E+00	4.43E−02	1.56	6.52E−02	7.14E−03	0	0	
FBtr0078623	CG11459-RA	1.71	1.14E−01	1.76E−02	1.96	1.88E−03	1.88E−02	0	0	Cysteine-type endopeptidase activity
FBtr0290216	CG13012-RB	2.51	4.57E−04	5.98E−05	1.88	4.31E−03	1.17E−04	0	0	
FBtr0084553	CG13606-RA*	1.75	1.90E−01	1.34E−02	1.5	9.42E−02	1.55E−03	1	0	
FBtr0084316	CG13841-RA**	1.93	5.45E−02	7.80E−03	2.04	8.54E−04	6.08E−04	2	1	
FBtr0339499	CG14615-RB*	1.5	5.99E−01	3.11E−03	1.58	5.56E−02	1.10E−03	4	0	Acyltransferase activity
FBtr0073111	CG14963-RA	2	2.44E−02	4.01E−06	1.82	7.27E−03	3.30E−04	0	0	
FBtr0307187	CG15202-RB*	1.6	3.77E−01	6.98E−03	1.81	8.17E−03	2.71E−05	3	1	
FBtr0080785	CG15255-RA	1.64	3.13E−01	4.60E−03	1.97	1.74E−03	1.76E−04	2	2	Metalloendopeptidase activity
FBtr0085456	CG15506-RA*	1.98	2.94E−02	1.46E−04	1.54	7.26E−02	4.01E−04	1	1	
FBtr0306579	CG17574-RE NC	1.69	2.81E−01	1.95E−02	1.66	3.06E−02	1.28E−03	1	1	
FBtr0306580	CG17574-RF	1.6	3.35E−01	3.12E−05	1.58	5.83E−02	1.69E−03	1	1	
FBtr0306581	CG17574-RG	1.5	6.54E−01	1.12E−02	1.55	7.04E−02	1.66E−04	1	1	
FBtr0082360	CG17734-RA*	1.8	9.58E−02	1.61E−04	2.09	5.18E−04	3.94E−05	2	1	
FBtr0073574	CG1806-RA	1.6	3.09E−01	3.99E−05	1.86	5.13E−03	1.25E−05	0	0	
FBtr0076388	CG18179-RA	2.99	9.96E−01	3.40E−02	2.24	9.94E−05	6.64E−03	0	0	Serine-type endopeptidase activity
FBtr0071678	CG30285-RA NC	1.56	4.35E−01	5.83E−04	2.03	9.41E−04	1.04E−04	2	1	
FBtr0070836	CG3097-RA**	1.73	1.54E−01	4.96E−08	1.72	1.89E−02	1.15E−05	2	2	Metallocarboxypeptidase activity
FBtr0333421	CG31704-RB NC	1.59	1.00E+00	3.64E−02	1.75	1.38E−02	3.46E−04	3	1	Serine-type endopeptidase inhibitor activity
FBtr0073030	CG32280-RA**	1.54	4.62E−01	4.72E−04	1.69	2.43E−02	3.34E−04	2	1	
FBtr0077032	CG32407-RA*	2.2	5.14E−03	1.94E−06	1.88	4.36E−03	2.21E−06	1	1	
FBtr0330118	CG32407-RB	2.09	1.16E−02	2.62E−06	1.92	2.98E−03	3.49E−06	1	1	
FBtr0077183	CG32523-RA**	2.14	7.94E−03	5.19E−04	2.45	8.28E−06	1.74E−04	2	0	Serine-type endopeptidase activity
FBtr0074184	CG32581-RA**	7.7	1.62E−21	3.38E−07	4.3	2.28E−15	1.28E−08	3	0	Zinc ion binding
FBtr0113439	CG32581-RB	3.3	4.62E−07	1.45E−05	3.16	1.81E−09	2.28E−07	3	0	Zinc ion binding
FBtr0112760	CG34454-RA**	1.52	5.09E−01	9.99E−04	2.12	3.75E−04	1.82E−03	1	0	Serine-type endopeptidase inhibitor activity
FBtr0301809	CG40198-RB	1.54	9.83E−01	3.23E−02	1.68	2.74E−02	1.88E−04	0	0	
FBtr0071854	CG4269-RA NC	1.53	4.60E−01	6.86E−03	2.24	9.81E−05	1.14E−02	3	1	
FBtr0303818	CG42808-RA**	2.06	1.98E−02	2.04E−03	2.33	3.57E−05	3.63E−06	1	1	
FBtr0303830	CG42824-RANC	1.51	5.50E−01	5.55E−04	1.5	9.42E−02	2.82E−03	0	0	
FBtr0304640	CG43057-RA NC	1.71	1.60E−01	7.41E−04	1.98	1.53E−03	4.80E−05	1	0	
FBtr0332368	CG43057-RB	1.54	4.90E−01	3.90E−03	1.62	4.19E−02	2.40E−03	3	0	
FBtr0075157	CG5506-RA**	1.67	2.80E−01	2.40E−02	2.65	8.70E−07	9.82E−06	1	0	
FBtr0085114	CG5909-RA	1.62	2.90E−01	1.57E−02	2.04	8.52E−04	8.29E−04	1	1	Serine-type endopeptidase activity
FBtr0336972	CG5921-RE	1.69	1.00E+00	3.64E−02	1.51	9.27E−02	1.63E−02	0	0	
FBtr0070861	CG6041-RA**	1.97	3.78E−02	2.63E−03	2.06	6.67E−04	2.80E−05	2	0	Serine-type endopeptidase activity
FBtr0087044	CG6429-RA*	1.57	4.22E−01	6.28E−03	2.4	1.45E−05	7.44E−05	2	0	Lysozyme activity
FBtr0079532	Sirup	1.64	3.02E−01	2.40E−03	2.08	5.83E−04	1.26E−04	1	0	
FBtr0100151	CG7224-RB NC	1.85	6.38E−02	3.37E−03	2.29	5.74E−05	6.33E−05	1	0	
FBtr0079143	CG9029-RA**	1.74	1.43E−01	2.14E−04	1.97	1.74E−03	1.57E−07	1	0	
FBtr0074026	CG9095-RA	1.65	2.36E−01	1.56E−03	1.8	8.63E−03	1.17E−03	3	0	Carbohydrate binding
FBtr0112984	CG9095-RB	1.71	2.36E−01	2.08E−02	1.83	6.77E−03	4.51E−05	3	0	Carbohydrate binding
FBtr0330402	CG9095-RC**	1.57	3.81E−01	7.82E−03	1.7	2.26E−02	5.94E−03	4	0	Carbohydrate binding
FBtr0074060	CG9240-RA	1.7	1.89E−01	2.22E−05	1.58	5.74E−02	7.93E−04	0	0	Serine-type peptidase activity
FBtr0074288	CG9782-RA**	1.69	2.69E−01	2.11E−02	2.49	5.86E−06	2.48E−06	1	0	
FBtr0086168	CheB42a-RA	1.57	4.01E−01	2.95E−04	1.5	9.56E−02	5.68E−03	0	0	Lipid binding
FBtr0076455	Cpr67B-RA**	3.29	5.96E−07	5.74E−05	2.6	1.52E−06	5.18E−06	1	1	Structural constituent of chitin-based cuticle
FBtr0076305	ect-RA**	3.89	2.92E−09	7.54E−06	2.86	6.92E−08	7.21E−05	6	4	Tube development?
FBtr0076307	ect-RB	2.88	5.15E−06	1.53E−04	2.96	2.05E−08	3.20E−03	6	4	Tube development?
FBtr0301385	ect-RD**	2.91	1.22E−05	1.41E−06	2.32	4.07E−05	2.66E−04	12	6	Tube development?
FBtr0087145	Hmgs-RA NC	1.56	4.20E−01	4.64E−05	1.96	2.00E−03	3.88E−05	3	3	Hydroxymethylglutaryl-CoA synthase activity
FBtr0087146	Hmgs-RC	1.71	1.73E−01	1.86E−04	1.55	7.12E−02	9.90E−04	3	3	Hydroxymethylglutaryl-CoA synthase activity
FBtr0080093	Lip4-RA**	1.58	3.66E−01	3.46E−03	2.6	1.48E−06	1.61E−04	3	1	Triglyceride lipase activity
FBtr0331672	Lip4-RC	1.53	5.15E−01	1.05E−02	2.4	1.46E−05	2.60E−05	5	2	Triglyceride lipase activity
FBtr0080934	LSm7-RA*	1.8	9.43E−02	1.02E−02	1.67	2.85E−02	6.31E−03	2	0	Spliceosome component?
FBtr0072633	LysP-RA	2.51	7.16E−05	7.74E−03	1.85	5.51E−03	4.67E−06	0	0	Lysozyme activity
FBtr0332521	mol-RG	1.64	2.58E−01	9.40E−04	1.63	4.04E−02	3.48E−04	2	0	Protein binding
FBtr0306737	obst-A-RB*	1.75	1.45E−01	9.09E−04	1.64	3.52E−02	2.82E−04	1	0	Structural constituent of peritrophic membrane
FBtr0078591	Osi24-RA**	3.74	1.32E−08	3.03E−04	2.21	1.39E−04	2.73E−04	3	1	
FBtr0300291	PGRP-LC-RE	2.53	2.96E−04	5.80E−05	1.53	7.87E−02	1.01E−02	0	0	Peptidoglycan receptor activity
FBtr0085689	PH4alphaMP-RA*	1.52	5.04E−01	5.16E−03	1.57	6.08E−02	3.61E−03	1	0	Procollagen-proline 4-dioxygenase activity
FBtr0070849	Rab18-RA**	1.53	5.17E−01	8.42E−04	2.14	2.87E−04	4.08E−05	3	1	GTP binding
FBtr0308131	sd-RM**	1.55	4.58E−01	1.15E−04	2.12	3.55E−04	2.95E−07	9	3	Sequence-specific DNA-binding transcription factor activity
FBtr0305663	Skeletor-RB**	2.58	1.98E−04	2.51E−04	2.81	1.37E−06	5.54E−06	3	3	Dopamine β-monooxygenase activity
FBtr0100125	vir-1-RD*	1.63	2.69E−01	3.14E−03	1.85	5.58E−03	2.17E−05	4	2	Virus-induced RNA

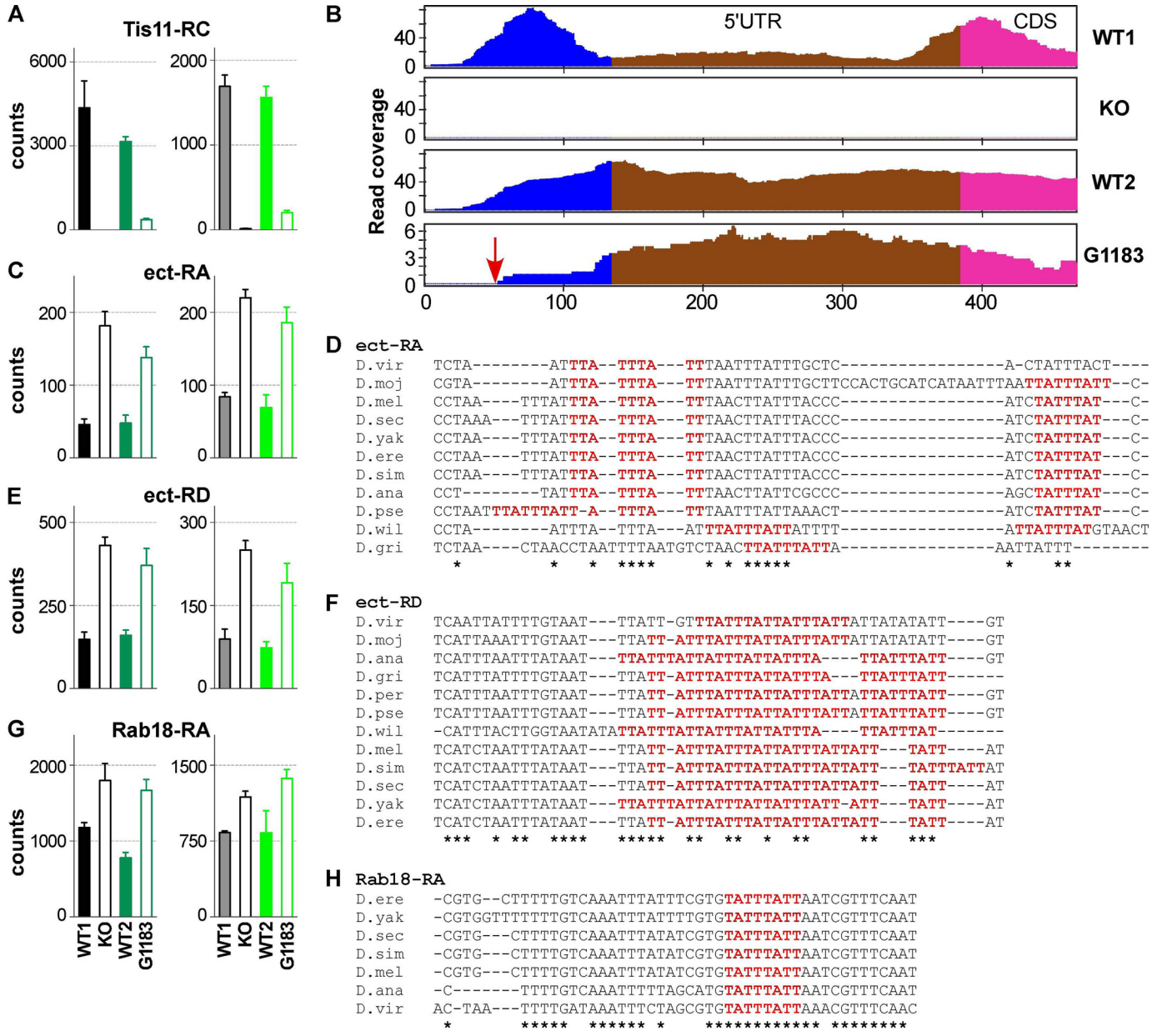

FIGURE 6. **Transcript expression determined by mRNASeq in WT, null, and *G1183* flies.** In the *left panel* of *A* are shown the average read count totals for the Tis11-RC mRNA, demonstrating its lack of expression in the null flies, as expected, and its decreased expression by ~8.6-fold in the *G1183* flies. The *right panel* of *A* shows NanoString quantitation of a subset of the original RNA samples used for mRNASeq, in which four samples were used in each group, except for "KO," which used three samples. *B* shows the average depth of read coverage for the 5′-end of the Tis11-RC transcript from the mRNASeq data from the four groups of flies. *Each panel* in *B* represents average depth of read coverage from all four biological samples used for that set. The contributions of the two exons comprising the 5′-UTR are shown in *blue* and *brown*, respectively, with the 5′-end of the protein coding sequence (*CDS*) shown in *pink*; this is also encoded by the second exon. The *arrow* points to the site of the *EP* element insertion in the *G1183* genome. There were no detectable transcript reads 5′ of this site. Note that the *vertical axis* in the *fourth panel* is *10-fold expanded* compared with the other three. Shown in the *left panels* of *C* and *E* are the means ± S.D. (*error bars*) of the mRNASeq expression results from two ect transcript variants, ect-RA and ect-RD, which have different 3′-UTRs; data from the NanoString analysis of a subset of these samples are shown in the *right panels* of *C* and *E*. The potential TTP family member binding sites in these transcripts are shown in *D* and *F*, respectively, and only show sequences that are conserved among the *Drosophila* species contained in the "classical" tree described in FlyBase. The optimum TTP binding heptamers, UAUUUAU, are highlighted in *red*. Identical residues at each position are indicated by *asterisks*. In the *left panel* of *G* are shown the mRNASeq expression data for Rab18 mRNA, encoding a small GTPase, whose 3′-UTR contains only a single heptamer binding site, with the corresponding NanoString data in the *right panel* of *G*. The potential TTP family member binding site in this transcript was less well conserved than seen with the other potential targets in this figure in some of the evolutionarily more distant *Drosophila* species (*H*). In *A*, *C*, *E*, and *G*, the mutant means (*i.e.* KO and *G1183*) from both the mRNASeq and NanoString analyses were statistically different from their respective WT means ($p < 0.01$ using Student's *t* test) in all cases.

more with $p < 0.05$ (Table 2). The largest changes were in the various isoforms of Tis11 mRNA. For Tis11-RC, the down-regulation was 4370-fold for the null flies over control, whereas the down-regulation was 8.6-fold in the *G1183* flies compared with the control flies (see Fig. 6*A*, *left*). These changes were confirmed by the NanoString assays. The Tis11-RC mRNA contains seven 7-mer potential Tis11 binding sites, scattered throughout its long 3′-UTR, suggesting that this transcript might itself be subject to autoregulation by its encoded protein. With this exception, none of the other down-regulated transcripts shown in Table 2 contained 7-mers of the UAUUUAU type.

TABLE 2

Transcripts down-regulated in adult *Tis11* null and hypomorphic males

The data shown here are from the two mRNASeq experiments described under "Materials and Methods." Column labels and other information are the same as in the legend to Table 1. Sdic1-RA, CG34166-RA, and CG40160-RA had two 5-mers, dob-RA had one 5-mer, and CG9317-RA had three 5-mers in their 3′-UTRs. Aside from Tis11-RC, none of these down-regulated transcripts contained UAUUUAU 7-mers in their 3′-UTRs. According to FlyBase, the longest Tis11 mRNA form, Tis11-RC, had a very long 3′-UTR (3317 bases) that contained 21 5-mers as well as six 7-mers, but the Tis11-RA isoform did not contain either motif.

FlyBase ID	Gene name	KO/ control	Max-P *p* value	*t* test *p* value	G1183/ control	Max-P *p* value	*t* test *p* value	GO molecular function or process
FBtr0075046	CG11619-RA	−1.68	1.48E−01	1.43E−03	−1.73	1.75E−02	1.58E−04	Glycerophosphodiesterase activity
FBtr0332306	CG1494-RB	−1.62	2.82E−01	9.52E−04	−1.71	2.12E−02	1.94E−05	ATPase activity
FBtr0290201	CG15553-RC	−3.93	5.81E−09	8.17E−04	−1.8	8.92E−03	2.11E−03	Transmembrane transporter activity
FBtr0074375	CG15865-RA	−1.97	3.14E−02	1.06E−03	−2.12	3.52E−04	1.99E−03	
FBtr0070050	CG32819-RA	−1.88	5.22E−02	2.12E−04	−1.54	7.32E−02	1.15E−04	Microtubule cytoskeleton organization
FBtr0070053	CG32820-RA	−1.97	2.59E−02	2.95E−04	−1.59	5.50E−02	1.53E−05	Microtubule cytoskeleton organization
FBtr0112357	CG34166-RA	−3.54	1.57E−08	1.34E−02	−1.91	3.00E−03	8.66E−03	
FBtr0301737	CG34166-RB	−3.08	6.51E−07	1.14E−02	−1.78	1.06E−02	9.24E−03	
FBtr0113813	CG40160-RA	−2.11	7.43E−03	2.27E−05	−1.6	4.80E−02	2.09E−03	Serine-type endopeptidase activity
FBtr0301802	CG40160-RE	−1.86	5.99E−02	1.22E−04	−1.55	6.80E−02	1.46E−04	Serine-type endopeptidase activity
FBtr0301803	CG40160-RF	−1.88	3.24E−02	1.06E−03	−1.59	5.16E−02	2.33E−03	Serine-type endopeptidase activity
FBtr0301804	CG40160-RG	−1.99	2.24E−02	2.58E−05	−1.56	6.74E−02	1.01E−03	Serine-type endopeptidase activity
FBtr0303833	CG42825-RA	−2.46	9.31E−01	2.66E−02	−1.56	3.16E−01	4.88E−02	Transmembrane transporter activity
FBtr0304142	CG42876-RA	−8.33	8.02E−16	4.36E−04	−2.15	2.62E−04	1.15E−03	
FBtr0083170	CG4525-RA	−2.72	6.23E−05	7.47E−04	−3.23	7.46E−10	6.20E−03	Cilium assembly
FBtr0302379	CG5999-RB	−2.37	1.72E−03	3.68E−04	−2.04	8.58E−04	2.90E−03	Glucuronosyltransferase activity
FBtr0302213	CG9150-RB	−3.44	3.09E−07	1.22E−03	−3.07	5.82E−09	1.19E−02	Oxidoreductase activity
FBtr0081395	CG9317-RA	−1.64	2.93E−01	2.11E−03	−1.68	2.58E−02	1.09E−02	Organic cation transporter activity
FBtr0073286	Claspin-RA	−2.12	2.33E−03	1.21E−02	−1.51	9.32E−02	1.38E−02	Mitotic DNA replication checkpoint
FBtr0073961	dob-RA	−1.86	5.57E−02	2.01E−03	−2.3	4.82E−05	5.58E−04	Lipid metabolic process
FBtr0075753	Hml-RA	−2.07	1.10E−02	6.31E−04	−1.62	2.93E−01	4.07E−02	Protein homodimerization activity
FBtr0333020	Hml-RB	−2.03	8.83E−03	3.70E−03	−1.7	2.33E−02	2.17E−02	Protein homodimerization activity
FBtr0089604	Sdic1-RA	−2.31	2.02E−03	7.23E−06	−1.5	9.52E−02	1.11E−03	Microtubule motor activity
FBtr0073683	Tis11-RA	−680	9.55E−201	5.56E−06	−8.35	1.02E−32	5.08E−06	3′-UTR-mediated mRNA destabilization
FBtr0073684	Tis11-RB	−411	6.04E−120	6.96E−07	−7.65	3.19E−30	1.02E−06	3′-UTR-mediated mRNA destabilization
FBtr0333756	Tis11-RC	−4370	0.00E+00	4.77E−05	−8.53	3.94E−33	3.88E−08	3′-UTR-mediated mRNA destabilization

DISCUSSION

We have begun to explore the functions of the *Drosophila* Tis11 protein in intact flies in order to unravel its role in the development and physiology of *Drosophila* and other insects. A long term goal is to use the advantages of the *Drosophila* system, including the fact that only a single TTP family member is expressed in this species, to help us understand the mechanisms of action of the entire TTP protein family in molecular and biochemical terms. We found that most of the biochemical characteristics of Tis11 were remarkably similar to those of its mammalian relatives. For example, when the protein was expressed in 293 cells or expressed in and purified from *E. coli*, it bound to the optimum target mRNA sequence as the mammalian proteins (*i.e.* UUAUUUAUU). This binding was dependent upon the presence of key cysteines and histidines within the TZF domain of the Tis11 protein and occurred with high affinity, with an apparent K_d of 2.3 nM, remarkably similar to that seen with a synthetic TZF domain from the human protein (35). Whether this is the optimum binding sequence for the fly protein remains to be determined. The Tis11 protein also caused the deadenylation and destabilization of target transcripts co-expressed in 293 cells in a manner similar to its mammalian counterparts, an effect that was at least partially abrogated by removal of a C-terminal, highly conserved sequence that, in human TTP, forms a binding site for the NOT1 protein and presumably its associated multiprotein complexes (19, 33), which include multiple deadenylases. Importantly, the same C-terminal sequence does not appear to contain the *Drosophila* nuclear export sequence (48), in contrast to what has been seen with some TTP family members in mammals (7, 47), thus allowing these two functional domains of the protein to be experimentally separable. These findings suggest that the functions of Tis11 in *Drosophila* are very similar to the functions of vertebrate TTP family members (*i.e.* to bind to AU rich elements in the 3′-UTRs of transcripts and to promote their destabilization, apparently by initially stimulating deadenylation).

A remarkable finding was that Tis11 could promote the decay of target RNAs in transfection studies in human cells, at amounts of transfected DNA similar to those used with an effective amount of the human TTP expression plasmid. Based on the alignment between the Tis11 TZF domains with those of the mammalian proteins and the effect of amino acid mutations of key residues within the Tis11 TZF domain to completely abrogate RNA binding, we can assume that the Tis11 TZF domain was involved in binding to mRNA targets in the human cells. Surprisingly, not only was the fly protein expressed in human cells largely intact, but it apparently managed to utilize the human cellular machinery to effect mRNA processing. This suggests that the fly protein can recruit the relevant human proteins to assemble one or more deadenylation complexes, with an example being the involvement of the highly conserved C-terminal putative NOT1 binding region in Tis11-promoted mRNA decay. It is striking that the TZF domain and the putative NOT1 binding domain were the only regions of the protein that were highly conserved among insects and also were highly conserved with the human TTP family members. It seems possible that these two sequence regions, separated by non-conserved sequences, might be sufficient to promote TTP-like mRNA deadenylation and turnover.

To begin to elucidate the normal role of this protein in *Drosophila* physiology and development, we examined the effects of its loss of function on mRNA levels in adult male flies. The *G1183* allele, in which an *EP* transposon was inserted into the first exon and interrupted the 5′-UTR, caused a decrease in Tis11 mRNA expression by more than 8-fold. *G1183* homozygotes were viable and fertile. A

completely separate genetic model resulted in complete Tis11 deficiency, and these flies were also viable and fertile. These two independently derived Tis11-deficient models allowed for the identification of higher probability direct Tis11 targets than could be identified in either model alone. Neither of these models is optimal. In the case of the null flies, in which a large deletion in the X chromosome is partially compensated for by a duplication, Tis11 mRNA expression was completely abolished. Expression of the immediately flanking genes was normal, but there was diminished expression of several more distant neighboring genes, presumably by the phenomenon of position effect variegation (52). The *G1183* allele resulted in an 8–9-fold decrease in Tis11 mRNA levels but did not seem to affect the expression of the immediate flanking genes in adult males. Nonetheless, the significantly affected potential target transcripts that were seen in both fly stocks suggest that at least some of them are likely to be due to the Tis11 deficiency held in common by the two stocks, either directly or as downstream effects.

In each stock, large numbers of transcripts accumulated abnormally in the Tis11-deficient adults, suggesting their possible identity as Tis11 target transcripts. However, only 69 transcripts were elevated in both stocks at a level of 1.5-fold or more, and $p < 0.05$. Many of these were confirmed as increased in one or both stocks using a separate RNA quantitation assay. Half of the up-regulated transcripts contained potential TTP family member binding sites in their 3′-UTRs, and many of those were conserved among other *Drosophila* species. The likelihood is that some of these up-regulated transcripts are direct Tis11 targets, whereas others were elevated as a secondary consequence of Tis11 deficiency; future work will be necessary to distinguish between these two possibilities. Future experiments will also be necessary to reconcile the large number of transcript changes that occurred in each model that were not shared by the other model.

Recent developmental expression analyses have demonstrated that high levels of Tis11 transcripts were observed throughout embryogenesis, particularly very early and quite late, and in early adulthood. This information suggests that comparisons between the WT and Tis11-deficient strains during embryogenesis might be particularly informative. These analyses also found that in larvae, the highest expression level was seen in the trachea, whereas in adults, the highest level was seen in the virgin spermatheca. Unfortunately, despite the fact that our antiserum directed at the intact protein reacted strongly in Western blots using the recombinant protein at high antibody dilutions (*e.g.* 1:10,000), we have not succeeded in using this antibody to identify the endogenous Tis11 protein, either in Western blots of one- or two-dimensional gels or in tissue immunostaining. Further work will be necessary for the complete characterization of endogenous Tis11 protein expression patterns.

An interesting example of a potential direct target transcript is encoded by *ect.* The predicted protein from this gene was initially described as a mouse interferon α-like protein based on the similarity of the AU-rich region in the 3′-UTRs of the two sequences (53). However, the encoded proteins do not resemble interferon and have no known function. *ect* is known to be expressed during mid-embryogenesis, especially in the ectodermal tissues of the embryo (54); this pattern of expression was confirmed by recent analyses. The same report described negligible expression during adulthood in both males and females. In our studies, ect transcripts were present at low levels in the control flies but were strongly up-regulated in both types of Tis11-deficient flies. The various transcripts of this gene contain several ideal potential binding sites for Tis11, and many of these are conserved in *ect* orthologues from other *Drosophila* species. We propose that the Tis11 protein may play a role in destabilizing ect transcripts; it will very interesting to examine this possibility during developmental stages when both transcripts are relatively highly expressed (*e.g.* in embryos). Studies to examine the effects of Tis11 deficiency at various developmental stages are currently under way.

In previous work, Dorner *et al.* (26) used a genome-wide RNAi approach in cultured *Drosophila* cells to determine that Tis11 was a major component in the RNAi pathway in this system. Our data do not shed light on this possibility. More recently, three papers described a role for the Tis11 protein in the regulation of the ARE-containing mRNA encoding the CecA1 antimicrobial peptide after stimulation of the innate immune system (25, 27, 29). In our mRNASeq analysis of mRNAs from adults, the CecA1-RA mRNA was up-regulated 2.8-fold in the *G1183* flies ($p = 0.03$) compared with control, but it was not significantly elevated in the null flies compared with control. In the NanoString confirmation assay, there was a significant increase in the null flies but not in the *G1183* flies. The CecA1-RA mRNA was fairly highly expressed in the adult males flies used here, with average RPKM values of 39.9 in the WT flies. For comparison, Tis11-RC had an average value of 17.6 in the same samples, and the 5th percentile value for this data set was 1.46. It will be of interest to examine the effects of *Tis11* deficiency on the levels and turnover of this transcript after innate immune system stimulation in adult flies. A role for Tis11 in the decay of the transcript encoding eya (eyes-absent) was also described very recently in S2 cell experiments (30); however, we did not see significant increases in eya transcripts in either deep sequencing analysis of the Tis11-deficient adults. In contrast to CecA1-RA, the eya-RB transcript (the highest expressing transcript variant) was poorly expressed in the adults, with an average RPKM in the WT flies of 2.7.

Recently, Spasic *et al.* (28) examined the *Drosophila* transcriptome for AU-rich elements and used a dsRNA approach in *Drosophila* SL2 cells to search for transcripts up-regulated in response to Tis11 knockdown. They identified 53 transcripts that were up-regulated more than 1.41-fold in the Tis11-deficient cells. Remarkably, there was only overlap of a single transcript between these 53 and the 69 transcripts identified in the current experiments as up-regulated in both types of Tis11-deficient adult flies. The common transcript was the vir-1 mRNA, which is induced in response to certain viral infections (55). It was significantly up-regulated by 1.63-fold in the null/control comparison and by 1.85-fold in the *G1183*/control comparison. Its 3′-UTR contains two 7-mer potential binding sites that are conserved in several other *Drosophila* species. The difference in results when comparing our mRNASeq data with the microarray data of Spasic *et al.* (28) raises the possibility that the SL2 cells, derived from late stage *Drosophila* embryos, might be a more appropriate model for embryonic Tis11 activity than for the activity in the adult fly, a possibility that can be

addressed in future experiments. However, we should emphasize that many other transcripts were up-regulated in one or the other of our comparisons but not both, and it seems likely that some of these overlap with the set of up-regulated transcripts identified by Spasic *et al.* (28).

Many mammalian ARE-binding proteins appear to have orthologues in *Drosophila*, but their potential interactions with Tis11 are not known. For example, the four AUF1 isoforms in humans (also known as heterogeneous nuclear ribonucleoprotein D0 proteins, or HNRPD proteins) appear to be orthologous to several isoforms of the *Drosophila* Squid proteins. We recently showed that two of the four human AUF1 isoforms can interact directly with the TZF domains of TTP family proteins, and this binding appears to potentiate the ability of TTP to bind to RNA (56). The TTP binding site within the AUF1 proteins is the so-called GY region near the C terminus; interestingly, several of the *Drosophila* isoforms have a similar GY-rich region in the same location, which is conserved in other insects. This raises the possibility that this particular interaction could be conserved between mammals and flies, a prospect that can be tested experimentally. Other ARE-binding proteins in flies include several isoforms of the ELAV (embryonic lethal abnormal vision) proteins, whose orthologues are the ELAV-like proteins 1–4 in humans (also known as HuA, HuB, HuR, etc. proteins in mammals). Both ELAV and HuD, when expressed ectopically in *Drosophila*, appeared to prevent the decay of AU-rich element-containing transcripts that were also expressed ectopically (57). Chen *et al.* (58) showed that ELAV can bind to the 3′-UTR of diptericin mRNA; this gene is rapidly and transiently expressed following immune stimulation. ELAV was later shown to be involved in splicing of AU-rich containing introns (59). HuD was found to bind to AREs within the LIM only domain protein 4 (LMO4) mRNA in response to ATP, resulting in increased stability of the LMO4 mRNA (60). To our knowledge, neither the potential interactions of these ARE-binding proteins with Tis11 nor their possible genetic interactions have been explored in *Drosophila*.

In conclusion, we have found that the biochemical properties of the *Drosophila* Tis11 protein are remarkably similar to those of its mammalian relatives, despite sequence conservation of only the RNA binding domains and the putative C-terminal NOT1 binding domains. In adult flies, two genetic models of Tis11 deficiency yielded many abnormally accumulating transcripts, many of which contained highly conserved potential Tis11 binding sites and which may well represent physiological targets for Tis11. Future studies will explore the effects of Tis11 deficiency on gene expression during various developmental stages in flies as well as the effects of infectious agents and other environmental stimuli on the possible Tis11 modulation of target transcript responses.

Acknowledgments—We are grateful to Essie Jones for stock maintenance and the Bloomington Drosophila Stock Center for stocks. We also thank the staff of the National Institutes of Health (NIH) Intramural Sequencing Center; the NIEHS, NIH, NanoString Core for dedicated assistance; and Drs. Ashley Godfrey and Daniel Menendez for helpful comments on the manuscript. We also thank Drs. Jasmin Raufer and Luke Alphey for generous assistance during the inception of this project.

REFERENCES

1. Shaw, G., and Kamen, R. (1986) A conserved AU sequence from the 3′ untranslated region of GM-CSF mRNA mediates selective mRNA degradation. *Cell* **46,** 659–667
2. Bakheet, T., Williams, B. R., and Khabar, K. S. (2003) ARED 2.0: an update of AU-rich element mRNA database. *Nucleic Acids Res.* **31,** 421–423
3. Chen, C. Y., and Shyu, A. B. (1995) AU-rich elements: characterization and importance in mRNA degradation. *Trends Biochem. Sci.* **20,** 465–470
4. Blackshear, P. J. (2002) Tristetraprolin and other CCCH tandem zinc-finger proteins in the regulation of mRNA turnover. *Biochem. Soc. Trans.* **30,** 945–952
5. Brooks, S. A., and Blackshear, P. J. (2013) Tristetraprolin (TTP): interactions with mRNA and proteins, and current thoughts on mechanisms of action. *Biochim. Biophys. Acta* **1829,** 666–679
6. Ciais, D., Cherradi, N., and Feige, J. J. (2013) Multiple functions of tristetraprolin/TIS11 RNA-binding proteins in the regulation of mRNA biogenesis and degradation. *Cell. Mol. Life Sci.* **70,** 2031–2044
7. Frederick, E. D., Ramos, S. B., and Blackshear, P. J. (2008) A unique C-terminal repeat domain maintains the cytosolic localization of the placenta-specific tristetraprolin family member ZFP36L3. *J. Biol. Chem.* **283,** 14792–14800
8. Blackshear, P. J., Lai, W. S., Kennington, E. A., Brewer, G., Wilson, G. M., Guan, X., and Zhou, P. (2003) Characteristics of the interaction of a synthetic human tristetraprolin tandem zinc finger peptide with AU-rich element-containing RNA substrates. *J. Biol. Chem.* **278,** 19947–19955
9. Worthington, M. T., Pelo, J. W., Sachedina, M. A., Applegate, J. L., Arseneau, K. O., and Pizarro, T. T. (2002) RNA binding properties of the AU-rich element-binding recombinant Nup475/TIS11/tristetraprolin protein. *J. Biol. Chem.* **277,** 48558–48564
10. Hudson, B. P., Martinez-Yamout, M. A., Dyson, H. J., and Wright, P. E. (2004) Recognition of the mRNA AU-rich element by the zinc finger domain of TIS11d. *Nat. Struct. Mol. Biol.* **11,** 257–264
11. Taylor, G. A., Carballo, E., Lee, D. M., Lai, W. S., Thompson, M. J., Patel, D. D., Schenkman, D. I., Gilkeson, G. S., Broxmeyer, H. E., Haynes, B. F., and Blackshear, P. J. (1996) A pathogenetic role for TNFα in the syndrome of cachexia, arthritis, and autoimmunity resulting from tristetraprolin (TTP) deficiency. *Immunity* **4,** 445–454
12. Stumpo, D. J., Byrd, N. A., Phillips, R. S., Ghosh, S., Maronpot, R. R., Castranio, T., Meyers, E. N., Mishina, Y., and Blackshear, P. J. (2004) Chorioallantoic fusion defects and embryonic lethality resulting from disruption of Zfp36L1, a gene encoding a CCCH tandem zinc finger protein of the Tristetraprolin family. *Mol. Cell. Biol.* **24,** 6445–6455
13. Ramos, S. B., Stumpo, D. J., Kennington, E. A., Phillips, R. S., Bock, C. B., Ribeiro-Neto, F., and Blackshear, P. J. (2004) The CCCH tandem zinc-finger protein Zfp36l2 is crucial for female fertility and early embryonic development. *Development* **131,** 4883–4893
14. Stumpo, D. J., Broxmeyer, H. E., Ward, T., Cooper, S., Hangoc, G., Chung, Y. J., Shelley, W. C., Richfield, E. K., Ray, M. K., Yoder, M. C., Aplan, P. D., and Blackshear, P. J. (2009) Targeted disruption of Zfp36l2, encoding a CCCH tandem zinc finger RNA-binding protein, results in defective hematopoiesis. *Blood* **114,** 2401–2410
15. Blackshear, P. J., Phillips, R. S., Ghosh, S., Ramos, S. B., Richfield, E. K., and Lai, W. S. (2005) Zfp36l3, a rodent X chromosome gene encoding a placenta-specific member of the Tristetraprolin family of CCCH tandem zinc finger proteins. *Biol. Reprod.* **73,** 297–307
16. Lai, W. S., Carballo, E., Thorn, J. M., Kennington, E. A., and Blackshear, P. J. (2000) Interactions of CCCH zinc finger proteins with mRNA. Binding of tristetraprolin-related zinc finger proteins to AU-rich elements and destabilization of mRNA. *J. Biol. Chem.* **275,** 17827–17837
17. Lai, W. S., Stumpo, D. J., Kennington, E. A., Burkholder, A. B., Ward, J. M., Fargo, D. L., and Blackshear, P. J. (2013) Life without TTP: apparent absence of an important anti-inflammatory protein in birds. *Am. J. Physiol. Regul. Integr. Comp. Physiol.* **305,** R689–R700
18. De, J., Lai, W. S., Thorn, J. M., Goldsworthy, S. M., Liu, X., Blackwell, T. K., and Blackshear, P. J. (1999) Identification of four CCCH zinc finger proteins in *Xenopus*, including a novel vertebrate protein with four zinc fingers and severely restricted expression. *Gene* **228,** 133–145
19. Blackshear, P. J., and Perera, L. (2014) Phylogenetic distribution and evo-

lution of the linked RNA-binding and NOT1-binding domains in the tristetraprolin family of tandem CCCH zinc finger proteins. *J. Interferon Cytokine Res.* **34,** 297–306
20. Puig, S., Askeland, E., and Thiele, D. J. (2005) Coordinated remodeling of cellular metabolism during iron deficiency through targeted mRNA degradation. *Cell* **120,** 99–110
21. Thompson, M. J., Lai, W. S., Taylor, G. A., and Blackshear, P. J. (1996) Cloning and characterization of two yeast genes encoding members of the CCCH class of zinc finger proteins: zinc finger-mediated impairment of cell growth. *Gene* **174,** 225–233
22. Wells, M. L., Huang, W., Li, L., Gerrish, K. E., Fargo, D. C., Ozsolak, F., and Blackshear, P. J. (2012) Posttranscriptional regulation of cell-cell interaction protein-encoding transcripts by Zfs1p in *Schizosaccharomyces pombe*. *Mol. Cell. Biol.* **32,** 4206–4214
23. Cuthbertson, B. J., Liao, Y., Birnbaumer, L., and Blackshear, P. J. (2008) Characterization of zfs1 as an mRNA-binding and -destabilizing protein in *Schizosaccharomyces pombe*. *J. Biol. Chem.* **283,** 2586–2594
24. Ma, Q., Wadleigh, D., Chi, T., and Herschman, H. (1994) The *Drosophila* TIS11 homologue encodes a developmentally controlled gene. *Oncogene* **9,** 3329–3334
25. Cairrao, F., Halees, A. S., Khabar, K. S., Morello, D., and Vanzo, N. (2009) AU-rich elements regulate *Drosophila* gene expression. *Mol. Cell. Biol.* **29,** 2636–2643
26. Dorner, S., Lum, L., Kim, M., Paro, R., Beachy, P. A., and Green, R. (2006) A genomewide screen for components of the RNAi pathway in *Drosophila* cultured cells. *Proc. Natl. Acad. Sci. U.S.A.* **103,** 11880–11885
27. Lauwers, A., Twyffels, L., Soin, R., Wauquier, C., Kruys, V., and Gueydan, C. (2009) Post-transcriptional regulation of genes encoding anti-microbial peptides in *Drosophila*. *J. Biol. Chem.* **284,** 8973–8983
28. Spasic, M., Friedel, C. C., Schott, J., Kreth, J., Leppek, K., Hofmann, S., Ozgur, S., and Stoecklin, G. (2012) Genome-wide assessment of AU-rich elements by the AREScore algorithm. *PLoS Genet.* **8,** e1002433
29. Wei, Y., Xiao, Q., Zhang, T., Mou, Z., You, J., and Ma, W. J. (2009) Differential regulation of mRNA stability controls the transient expression of genes encoding *Drosophila* antimicrobial peptide with distinct immune response characteristics. *Nucleic Acids Res.* **37,** 6550–6561
30. Yeh, P. A., Yang, W. H., Chiang, P. Y., Wang, S. C., Chang, M. S., and Chang, C. J. (2012) *Drosophila* eyes absent is a novel mRNA target of the tristetraprolin (TTP) protein DTIS11. *Int. J. Biol. Sci.* **8,** 606–619
31. Lai, W. S., Carballo, E., Strum, J. R., Kennington, E. A., Phillips, R. S., and Blackshear, P. J. (1999) Evidence that tristetraprolin binds to AU-rich elements and promotes the deadenylation and destabilization of tumor necrosis factor α mRNA. *Mol. Cell. Biol.* **19,** 4311–4323
32. Lai, W. S., Thompson, M. J., and Blackshear, P. J. (1998) Characteristics of the intron involvement in the mitogen-induced expression of Zfp-36. *J. Biol. Chem.* **273,** 506–517
33. Fabian, M. R., Frank, F., Rouya, C., Siddiqui, N., Lai, W. S., Karetnikov, A., Blackshear, P. J., Nagar, B., and Sonenberg, N. (2013) Structural basis for the recruitment of the human CCR4-NOT deadenylase complex by tristetraprolin. *Nat. Struct. Mol. Biol.* **20,** 735–739
34. Wilson, G. M. (2005) in *Reviews in Fluorescence 2005* (Geddes, C. D., and Lakowicz, J. R., eds) pp. 223–243, Springer Science+Business Media, Inc., New York
35. Brewer, B. Y., Malicka, J., Blackshear, P. J., and Wilson, G. M. (2004) RNA sequence elements required for high affinity binding by the zinc finger domain of tristetraprolin: conformational changes coupled to the bipartite nature of AU-rich MRNA-destabilizing motifs. *J. Biol. Chem.* **279,** 27870–27877
36. Jameson, D. M., and Sawyer, W. H. (1995) Fluorescence anisotropy applied to biomolecular interactions. *Methods Enzymol.* **246,** 283–300
37. Emsley, P., Lohkamp, B., Scott, W. G., and Cowtan, K. (2010) Features and development of Coot. *Acta Crystallogr. D Biol. Crystallogr.* **66,** 486–501
38. Duan, Y., Wu, C., Chowdhury, S., Lee, M. C., Xiong, G., Zhang, W., Yang, R., Cieplak, P., Luo, R., Lee, T., Caldwell, J., Wang, J., and Kollman, P. (2003) A point-charge force field for molecular mechanics simulations of proteins based on condensed-phase quantum mechanical calculations. *J. Comput. Chem.* **24,** 1999–2012
39. Pérez, A., Marchán, I., Svozil, D., Sponer, J., Cheatham, T. E., 3rd, Laughton, C. A., and Orozco, M. (2007) Refinement of the AMBER force field for nucleic acids: improving the description of α/γ conformers. *Biophys. J.* **92,** 3817–3829
40. Humphrey, W., Dalke, A., and Schulten, K. (1996) VMD: visual molecular dynamics. *J. Mol. Graphics* **14,** 33–38
41. Carballo, E., Lai, W. S., and Blackshear, P. J. (2000) Evidence that tristetraprolin is a physiological regulator of granulocyte-macrophage colony-stimulating factor messenger RNA deadenylation and stability. *Blood* **95,** 1891–1899
42. Rørth, P. (1996) A modular misexpression screen in *Drosophila* detecting tissue-specific phenotypes. *Proc. Natl. Acad. Sci. U.S.A.* **93,** 12418–12422
43. Livak, K. J., and Schmittgen, T. D. (2001) Analysis of relative gene expression data using real-time quantitative PCR and the $2(-\Delta\Delta C(T))$ method. *Methods* **25,** 402–408
44. Li, H., and Durbin, R. (2009) Fast and accurate short read alignment with Burrows-Wheeler transform. *Bioinformatics* **25,** 1754–1760
45. Huang, W., Umbach, D. M., Vincent Jordan, N., Abell, A. N., Johnson, G. L., and Li, L. (2011) Efficiently identifying genome-wide changes with next-generation sequencing data. *Nucleic Acids Res.* **39,** e130
46. Fortina, P., and Surrey, S. (2008) Digital mRNA profiling. *Nat. Biotechnol.* **26,** 293–294
47. Phillips, R. S., Ramos, S. B., and Blackshear, P. J. (2002) Members of the tristetraprolin family of tandem CCCH zinc finger proteins exhibit CRM1-dependent nucleocytoplasmic shuttling. *J. Biol. Chem.* **277,** 11606–11613
48. Twyffels, L., Wauquier, C., Soin, R., Decaestecker, C., Gueydan, C., and Kruys, V. (2013) A masked PY-NLS in *Drosophila* TIS11 and its mammalian homolog tristetraprolin. *PLoS One* **8,** e71686
49. Cao, H., Tuttle, J. S., and Blackshear, P. J. (2004) Immunological characterization of tristetraprolin as a low abundance, inducible, stable cytosolic protein. *J. Biol. Chem.* **279,** 21489–21499
50. Lai, W. S., Parker, J. S., Grissom, S. F., Stumpo, D. J., and Blackshear, P. J. (2006) Novel mRNA targets for tristetraprolin (TTP) identified by global analysis of stabilized transcripts in TTP-deficient fibroblasts. *Mol. Cell. Biol.* **26,** 9196–9208
51. Lai, W. S., Kennington, E. A., and Blackshear, P. J. (2003) Tristetraprolin and its family members can promote the cell-free deadenylation of AU-rich element-containing mRNAs by poly(A) ribonuclease. *Mol. Cell. Biol.* **23,** 3798–3812
52. Elgin, S. C., and Reuter, G. (2013) Position-effect variegation, heterochromatin formation, and gene silencing in *Drosophila*. *Cold Spring Harb. Perspect. Biol.* **5,** a017780
53. Nakanishi, Y., Paco-Larson, M. L., and Garen, A. (1986) DNA homology between the 3′-untranslated regions of a developmentally regulated *Drosophila* gene and a mouse α-interferon gene. *Gene* **46,** 79–88
54. Raha, D., Nguyen, Q. D., and Garen, A. (1990) Molecular and developmental analyses of the protein encoded by the *Drosophila* gene ectodermal. *Dev. Genet.* **11,** 310–317
55. Kemp, C., Mueller, S., Goto, A., Barbier, V., Paro, S., Bonnay, F., Dostert, C., Troxler, L., Hetru, C., Meignin, C., Pfeffer, S., Hoffmann, J. A., and Imler, J. L. (2013) Broad RNA interference-mediated antiviral immunity and virus-specific inducible responses in *Drosophila*. *J. Immunol.* **190,** 650–658
56. Kedar, V. P., Zucconi, B. E., Wilson, G. M., and Blackshear, P. J. (2012) Direct binding of specific AUF1 isoforms to tandem zinc finger domains of tristetraprolin (TTP) family proteins. *J. Biol. Chem.* **287,** 5459–5471
57. Toba, G., Qui, J., Koushika, S. P., and White, K. (2002) Ectopic expression of *Drosophila* ELAV and human HuD in *Drosophila* wing disc cells reveals functional distinctions and similarities. *J. Cell Sci.* **115,** 2413–2421
58. Chen, H. X., Li, Y., Jiang, Z. Z., Qu, X. M., Yang, S. L., and Ma, W. J. (2004) The existence of a putative post-transcriptional regulatory element in 3′-UTR of *Drosophila* antibacterial peptide diptericin's mRNA. *FEBS Lett.* **561,** 181–185
59. Soller, M., and White, K. (2005) ELAV multimerizes on conserved AU4–6 motifs important for ewg splicing regulation. *Mol. Cell. Biol.* **25,** 7580–7591
60. Chen, H. H., Xu, J., Safarpour, F., and Stewart, A. F. (2007) LMO4 mRNA stability is regulated by extracellular ATP in F11 cells. *Biochem. Biophys. Res. Commun.* **357,** 56–61